Molecular Biology of the Cell
Vol. 19, 1046–1061, March 2008

Nucleocytoplasmic Shuttling of the Golgi Phosphatidylinositol 4-Kinase Pik1 Is Regulated by 14-3-3 Proteins and Coordinates Golgi Function with Cell Growth

Lars Demmel,*† Mike Beck,*† Christian Klose,† Anne-Lore Schlaitz,† Yvonne Gloor,† Peggy P. Hsu,‡ Jan Havlis,†§ Andrej Shevchenko,† Eberhard Krause,‖ Yannis Kalaidzidis,†¶ and Christiane Walch-Solimena†

†Max Planck Institute of Molecular Cell Biology and Genetics, Dresden D-01307, Germany; ‡Whitehead Institute for Biomedical Research, Cambridge, MA 02142; ‖Mass Spectrometry Group, Leibniz Institute of Molecular Pharmacology, Berlin D-13125, Germany; and ¶A. N. Belozersky Institute of Physico-Chemical Biology, Moscow State University, Moscow 119899, Russia

Submitted February 16, 2007; Revised December 13, 2007; Accepted December 20, 2007
Monitoring Editor: Benjamin Glick

The yeast phosphatidylinositol 4-kinase Pik1p is essential for proliferation, and it controls Golgi homeostasis and transport of newly synthesized proteins from this compartment. At the Golgi, phosphatidylinositol 4-phosphate recruits multiple cytosolic effectors involved in formation of post-Golgi transport vesicles. A second pool of catalytically active Pik1p localizes to the nucleus. The physiological significance and regulation of this dual localization of the lipid kinase remains unknown. Here, we show that Pik1p binds to the redundant 14-3-3 proteins Bmh1p and Bmh2p. We provide evidence that nucleocytoplasmic shuttling of Pik1p involves phosphorylation and that 14-3-3 proteins bind Pik1p in the cytoplasm. Nutrient deprivation results in relocation of Pik1p from the Golgi to the nucleus and increases the amount of Pik1p–14-3-3 complex, a process reversed upon restored nutrient supply. These data suggest a role of Pik1p nucleocytoplasmic shuttling in coordination of biosynthetic transport from the Golgi with nutrient signaling.

INTRODUCTION

Phosphoinositides (PIs) are a family of lipids that include several derivatives distinguished by the phosphorylation status of their inositol headgroups. PIs play essential roles in the regulation of membrane traffic. The regulation of the activity and localization of PI kinases and phosphatases that modify PI headgroups is of central importance in the understanding of basic cellular processes such as secretion and growth or establishment of polarity.

The phosphatidylinositol 4-kinases (PI 4-kinase) Pik1p in yeast and PI 4-kinase IIIβ in vertebrates are found at the *trans*-Golgi network (TGN) (Godi *et al*., 1999; Walch-Solimena and Novick, 1999; Sciorra *et al*., 2005; Strahl *et al*., 2005), and they are key regulators of membrane transport and Golgi homeostasis. Mutants with defects in PI(4)P production by these lipid kinases showed reduced secretion, delayed vacuolar transport, defective protein retrieval from endosomes to the Golgi, and aberrant Golgi morphology (Godi *et al*., 1999; Hama *et al*., 1999; Walch-Solimena and Novick, 1999; Audhya *et al*., 2000). Recent work, mainly in mammalian cells, has revealed effectors of phosphatidylinositol 4-phosphate [PI(4)P] such as the PI(4)P adaptor proteins FAPP1 and FAPP2, which are involved in the generation of transport carriers for exocytosis (Godi *et al*., 2004; Vieira *et al*., 2005) and the clathrin adaptor AP-1 (Wang *et al*., 2003; Heldwein *et al*., 2004) that participates in the formation of clathrin-coated vesicles. In the mammalian system, Golgi PI(4)P is not only generated by the type IIIβ PI 4-kinase (Wong *et al*., 1997; Godi *et al*., 1999, 2004) but also by type IIα (Wei *et al*., 2002; Weixel *et al*., 2005).

In addition to their TGN localization, both Pik1p and PI 4-kinase IIIβ also localize to the nucleus (Garcia-Bustos *et al*., 1994; Walch-Solimena and Novick, 1999; de Graaf *et al*., 2002; Strahl *et al*., 2005). Although the nuclear function of the two PI 4-kinases remains unknown, it has been demonstrated that they undergo nucleocytoplasmic shuttling (de Graaf *et al*., 2002; Strahl *et al*., 2005). Reversible relocation of Pik1p from the nucleus to the cytoplasm has been observed upon block of secretion in several *sec* (secretion) mutants as part of the so-called "arrest of secretion response" (ASR) (Walch-Solimena and Novick, 1999; Nanduri and Tartakoff, 2001). However, the physiological significance and regulation of this process is not understood.

Nucleocytoplasmic shuttling is a behavior of many proteins, such as kinases, transcription factors, and cell cycle regulators (for review, see Nigg, 1997). There are several

This article was published online ahead of print in *MBC in Press* (http://www.molbiolcell.org/cgi/doi/10.1091/mbc.E07–02–0134) on January 2, 2008.

* These authors contributed equally to this work.

Present address: § Faculty of Science, Department of Analytical Chemistry, Masaryk University, Brno, Czech Republic.

Address correspondence to: Christiane Walch-Solimena (csolimena@mpi-cbg.de).

Abbreviations used: ASR, arrest of secretion response; λ-PPase, λ-protein phosphatase; GST, Glutathione S-transferase; PAP, peroxidase anti-peroxidase; PI, phosphoinositide; PI 4-kinase, phosphatidylinositol 4-kinase; PI(4)P, phosphatidylinositol 4-phosphate; TGN, *trans*-Golgi network; TAP, tandem affinity purification.

examples in which this shuttling process is regulated by 14-3-3 proteins, a family of phosphorylation-dependent chaperones. 14-3-3 proteins are ubiquitous and highly conserved proteins, which alter protein localization or activity, modify protein–protein interactions, and induce conformational changes of their targets (for reviews, see Muslin and Xing, 2000; Tzivion and Avruch, 2002; Yaffe, 2002; Dougherty and Morrison, 2004; van Heusden and Steensma, 2006). The 14-3-3 proteins play a role in cellular processes such as cell cycle regulation, apoptosis, and cell proliferation (for review, see Dougherty and Morrison, 2004). In yeast, the two 14-3-3 proteins Bmh1p and Bmh2p are redundant and in combination essential proteins. They have been shown to play a role in the polarization of the actin cytoskeleton, cell cycle regulation at the G1/S transition, and regulation of transcription factors involved in nutrient signaling (Lottersberger *et al*., 2006; van Heusden and Steensma, 2006).

The only currently known binding partner of Pik1p is the calmodulin-like protein frequenin-1 (Frq1p), which functions in binding of Pik1p to the Golgi (Hendricks *et al*., 1999; Ames *et al*., 2000; Strahl *et al*., 2005). We now report that Pik1p binds to the yeast 14-3-3 proteins Bmh1p and Bmh2p. The Pik1p–14-3-3 interaction requires phosphorylation, occurs primarily in the cytoplasm, and controls nucleocytoplasmic shuttling and availability of Pik1p for Golgi recruitment. This interaction interferes with secretion, because overexpression of *BMH2* results in a phenocopy of *pik1-101* mutant transport phenotypes in secretion. We further show that under nutrient deprivation the PI 4-kinase relocates from the TGN to the cytoplasm and into the nucleus. This relocation is rapidly reversed upon restoration of nutrient supply. Therefore, the nucleocytoplasmic shuttling of Pik1p and 14-3-3 interaction might be part of a regulatory circuit that coordinates cell growth cues with PI(4)P production at the TGN, possibly to adjust membrane transport to the growth requirements of the cell.

MATERIALS AND METHODS

Yeast Strains, Media, and Materials

The genotypes of the *Saccharomyces cerevisiae* strains used in this study are listed in Supplemental Table 2. Yeast strains were cultured in YPD, SC dropout media, or SD minimal media supplemented with necessary amino acids. Yeast were transformed using the lithium acetate method (Schiestl and Gietz, 1989). Yeast strain L40 was used for the two-hybrid system (*MATa*, *trp1-*, *ade2-*, *leu2-*, *his3-*, *LYS::LexA-HIS3*, *URA::LexA-LacZ*). Complete protease inhibitors were from Roche Diagnostics (Mannheim, Germany) and Zymolase 100-T was from MP Biomedicals (Irvine, CA). The anti-hemagglutinin (HA) antibody Y11 was obtained from Santa Cruz Biotechnology (Santa Cruz, CA). Polyclonal anti-green fluorescent protein (GFP) antibody (goat) was from the protein expression facility of the MPI-CBG (Dresden, Germany). Monoclonal anti-GFP antibody (clones 7.1 and 13.1) was from Roche Diagnostics.

Plasmid and Strain Constructions

Constructs used in this study are listed in Supplemental Table 3. General molecular biological methods were as described previously (Sambrook and Russel, 2001). Plasmid pMBL31 (LexA yeast two-hybrid vector) was constructed by replacing the *GAL4* DNA-binding domain of vector pGBKT7 (Clontech, Mountain View, CA) by the coding region of LexA flanked by *ADH* promoter and terminator as described for pMBL33 (Brickley *et al*., 2005). Fusion constructs with the *GAL4* DNA-binding domain and with LexA were obtained by in frame ligation of polymerase chain reaction (PCR) products. The *pik1*^{S396A} and *pik1*^{S396D} mutations have been generated by site-directed mutagenesis (QuikChange Multi kit; Stratagene, La Jolla, CA), and they were introduced into pRS415 containing the *ADH* promoter fused to *GFP* for N-terminal tagging. The *pik1-101* allele has been described previously (Walch-Solimena and Novick, 1999). The alleles *pik1-145-148* were generated by site-directed mutagenesis (QuikChange Multi kit; Stratagene) and contain S396A, S605A (*pik1-145*); S605A, S780A (*pik1-146*); S396A, S780A (*pik1-147*); and all three mutations (*pik1-148*). Allele *pik1-130* (H35R, T105M, D147G, M367T, N372S, R462G and F530Y) was obtained by error-prone PCR. Yeast strains genomically tagged with 3xHA, 13xMyc, or tandem affinity purification (TAP) tag were constructed as described previously (Longtine *et al*., 1998; Puig *et al*., 2001). In Pik1p-TAP (CSY370, CSY513, and YMB119), a SGPGS linker (TCTGGTCCATCTGGT) was inserted between the Pik1p and the TAP tag. The Frq1p-TAP strain was from Open Biosystems (Huntsville, AL). A GGSGG peptide linker (GGTGGTTCTGGTGGT) has been inserted between Bmh1p or Bmh2p and 13xMyc in the case of YMB054, YMB058, or YMB119. To create a Bmh1p-3xha fusion (YMB148), a SGPGS linker (TCTGGTCCATCTGGT) was inserted between the Bmh1p and the HA tag.

Interaction Assays Using the Yeast Two-Hybrid System

For two-hybrid interaction studies the *GAL4* based system Matchmaker 3′ (Clontech) and a LexA-system with a modified LexA vector were used as described previously (Brickley *et al*., 2005). For measurement of β-galactosidase activity in liquid culture, an *O*-nitrophenyl β-D-galactopyranoside (ONPG) solution assay was performed as described previously (Miller, 1972; Sambrook and Russel, 2001).

Glutathione S-transferase (GST) Pull-Down Assays

GST and GST-Bmh1/2p-fusions were expressed in *Escherichia coli* BL21. Cells were homogenized in phosphate-buffered saline (PBS) with protease inhibitors (Complete and phenylmethylsulfonyl fluoride [PMSF]) by sonication. Lysates were incubated with 1% Triton X-100 for 10 min at 4°C, cleared, and mixed with glutathione Sepharose 4B slurry (GE Healthcare, Chalfont St. Giles, United Kingdom). After binding for 10 min at room temperature, beads were harvested and washed twice with PBS (with protease inhibitors) and once with yeast lysis buffer (20 mM Tris-Cl, pH 7.5, 150 mM NaCl, 1 mM EDTA, 100 μM Na_3VO_4, 25 mM NaF, 1 mM PMSF, and Complete). Aliquots were used to pull down Pik1p from yeast lysate (corresponding to 5 OD units of cells) overnight at 4°C. Beads were washed with yeast lysis buffer; three times with 20 mM Tris-HCl, pH 7.5, 350 mM NaCl, 2 mM EDTA, and 0.1% NP-40; and once with PBS. Thirty microliters of supernatant and the resuspended beads were separated by SDS-polyacrylamide gel electrophoresis (PAGE) and analyzed by immunoblotting. In some experiments, the effects of adding phosphatase inhibitors (100 μM Na_3VO_4 and 25 mM NaF) and/or λ-PPase to yeast lysates were examined.

In vitro transcription/translation of Pik1p was performed using the TNT T7 Quick-Coupled Transcription/Translation System (Promega, Madison, WI), including [^{35}S]methionine (PerkinElmer Life and Analytical Sciences, Boston, MA) according to the manufacturer's instructions from plasmid pLD103. GST and GST-Bmh1/2p were expressed and solubilized as described above. Five hundred microliters of cleared *E. coli* lysate was incubated with 150 μl of prewashed 50% glutathione-Sepharose 4B slurry on a rotator for 30 min at room temperature.

To precipitate Pik1p, 40 μl of the TNT reaction mix was incubated overnight at 4°C with GST only beads or beads loaded with GST-Bmh1p or GST-Bmh2p, respectively. Samples were washed once with PBS, with washing buffer (10 mM Tris-HCl, pH 8.0, 2 mM EDTA, and 0.5% NP-40) containing 150 mM NaCl or 500 mM NaCl and once with 10 mM Tris-HCl, pH 8.0. Beads were resuspended in SDS-sample buffer and proteins were analyzed by SDS-PAGE followed by autoradiography.

TAP and Protein Identification

The strain CSY 370 was used for purification of Pik1p complexes and the Frq1p-TAP strain for Frq1p. TAP from 12 l of YPD culture was performed as described previously (Rigaut *et al*., 1999; Puig *et al*., 2001) with the modification that Complete protease inhibitors were used throughout the procedure. When indicated, extractions were performed in the presence of phosphatase inhibitors (25 mM NaF and 100 μM Na_3VO_4). Proteins were separated by SDS-PAGE (4–16% gradient) and visualized with Coomassie, and bands were excised and in-gel digested with trypsin and analyzed by a combination of matrix-assisted laser desorption ionization (MALDI) mass spectrometry (MS) peptide mapping and nanoelectrospray (nanoES) tandem mass spectrometry (MS/MS) as described previously (Shevchenko *et al*., 1996) by using, respectively, REFLEX IV MALDI time of flight (TOF) mass spectrometer (Bruker Daltonics, Bremen, Germany) and QSTAR Pulsar *i* hybrid quadrupole time-of-flight mass spectrometer (MDS Sciex, Concord, ON, Canada). Database searches were performed by Mascot, version 2.1 software (Matrix Science, London, United Kingdom) installed on a local server against the subset of *S. cerevisiae* proteins in MSDB protein sequence database.

Gap1p Activity Assay

The Gap1p activity was determined by measuring the uptake rate of [^{14}C]citrulline as described previously (Roberg *et al*., 1997).

Identification of Phosphorylation Sites by Mass Spectrometry

Phosphorylated Pik1p bands were excised. Disulfide bond reduction/alkylation, tryptic in-gel digestion, and sample preparation before analysis by MS were performed as described previously (Bauer and Krause, 2005). Separation of phosphorylated peptides was performed by selective binding on titanium

dioxide (Pinkse *et al*., 2004). Peptide samples (5 μl in 30% acetonitrile and 2% formic acid) were loaded on a TiO_2 column (5 μm, 100 Å; 5 mm × 300 μm i.d.) at a flow rate of 1.5 μl/min. After washing, the phosphopeptides were eluted with 0.1 M ammonium bicarbonate. The eluate was dried in a vacuum centrifuge and redissolved in 6 μl of 0.1% trifluoroacetic acid in acetonitrile: water (1:9, vol/vol). Liquid chromatography (LC)-MS and MS/MS experiments were performed on a quadrupole orthogonal acceleration time-of-flight mass spectrometer Q-TOF Ultima (Micromass, Manchester, United Kingdom). A CapLC liquid chromatography system (Waters, Milford, MA) was used to deliver the peptide solution to the nanoelectrospray source. Peptides were separated using a capillary column (PepMap C18; 3 μm, 100 Å; 150 mm × 75 μm i.d.; Dionex, Idstein, Germany) and an eluent flow rate of 200 nl/min. Mobile phase A was 0.1% formic acid in acetonitrile:water (3:97, vol/vol), and mobile phase B was 0.1% formic acid in acetonitrile:water (8:2, vol/vol). Runs were performed using a gradient of 4–65% B in 60 min. To perform MS/MS experiments, automatic function switching (survey scanning) was used. The processed MS/MS spectra (MassLynx version 4.0 software) were compared with the theoretical fragment ions of enzymatic fragments of Pik1p.

Live Cell Imaging

For the visual Gap1p trafficking assay, yeast strains transformed with TPQ99 [encoding Gap1p(K9A,K16A)-GFP fusion protein, called Gap1*p-GFP in the text, mutations according to Soetens *et al*. (2001)] were grown to early log phase in YP, containing 2% raffinose, and then reporter expression was induced by adding galactose to 3% for 3 h. For GFP–Pik1p microscopy, late log phase cultures were grown in SC-URA medium for 48 h. Early log phase cultures were grown to an OD_{600} of 0.3. Cells using glycerol as a carbon source were cultured for 3 d in YPG medium. To deplete glucose or glycerol from the medium, cells from early log phase cultures were harvested from SC-URA or YPG medium, respectively. Cells were washed twice with medium lacking carbon sources, and then they were resuspended in glucose or glycerol-free medium for 45 min. Cells were depleted of glucose (45 min) and at indicated times, glucose (2% final concentration) was added. Cells were then harvested and directly observed without fixation under a fluorescent microscope (Axioplan 2 MOT; Carl Zeiss, Jena, Germany).

Image Quantification

The images were processed with MotionTracking program: The background window size was chosen so that the fluorescence of cytosolic GFP pool was treated as a background. The background was calculated by modification of "dynamic" algorithm. The mean value and SD was calculated inside the square window. Then the mean value was recalculated but all intensities above mean + 2 were excluded from consideration. The last procedure was repeated four times. The mean values after this procedure well correspond to "background intensity," because the small bright structures were excluded from the averaging procedure. The intensities of small structures were fitted by hat-like analytical function:

$$I(x,y) = \sum \frac{A_i}{1 + \left\{ \left[\frac{((x - x_i)\cos(\alpha_i) - (y - y_i)\sin(\alpha_i)}{w_i} \right]^2 + \left[\frac{(x - x_i)\sin(\alpha_i) - (y - y_i)\cos(\alpha_i)}{h_i} \right]^2 \right\}^{pi}}$$

where A_i is intensity, x_i and y_i are center coordinates, w_i and h_i are width by two perpendicular dimensions, α_I is angle between main axes and the axes X/Y of image, p_i is power (sharpness) of function, the index i refers to ith particle. For details of the fitting procedure see Rink *et al*. (2005). The number of dotted structures was calculated inside every cell. Because the program could not well distinguish cells that are touching each other, the cell boundaries were drawn manually. The integral intensity of structures was calculated by analytical integration of fitting functions.

Immunofluorescence Microscopy

Immunofluorescence experiments were performed as described in Walch-Solimena *et al*. (1997). Images were acquired using a microscope (Zeiss Axiovert 200) equipped with a Plan-Apo 100×/1.4 oil objective or Zeiss Axioplan 2 MOT with a Plan-Neofluar 100×/1.3 oil objective (SPOT camera; Diagnostic Instruments, Sterling Heights, MI).

Cell Fractionation and Immunoprecipitation

Cell fractionation was performed as described previously (Du and Novick, 2001), with protease inhibitors (Complete) used throughout the procedure unless otherwise indicated. Equal volumes were analyzed by SDS-PAGE and immunoblotting. For immunoprecipitations from cellular fractions, membrane-bound and soluble fractions were prepared from yeast cells (YMB148) by 100,000 × *g* centrifugation for 45 min. All samples were then adjusted to 2 ml, Tween 20 was added to 0.5% final concentration, and samples incubated on ice for 30 min. After preadsorption with protein A-Sepharose, precipitation was carried out using anti-myc antibody (9E10), followed by protein A-Sepharose incubation for 2 h at 4°C. Beads were harvested, washed six times with cold 20 mM HEPES, pH 7.4, containing 200 mM KCl, 0.5 mM dithiothreitol (DTT), 2 mM EDTA, 10 mM NaF, 100 μM Na_3VO_4, and 0.5% Triton X-100 followed by two washes without detergent.

For glucose depletion experiments, yeast cultures (YMB148) were grown overnight in YPD to mid-log phase (OD_{600} = 0.8–1.0). Glucose depletion was performed as described above. Cells were then harvested, washed with washing buffer 1 (50 mM Tris-HCl, pH 7.5, and 10 mM NaN_3) and washing buffer 2 (20 mM Tris-HCl, pH 7.5), and resuspended in 1 ml of lysis buffer (50 mM Tris-HCl, pH 7.5, 150 mM KCl, 1 mM EDTA, 1 mM DTT, 0.1% Tween 20, and Complete). Cells were lysed using 2 g of Zirconia beads and a Mini-BeadBeater-8 (Biospec Products, Bartlesville, OK). The lysate was cleared by centrifugation (15 min; 14,000 × *g*; 4°C). Equal amounts of protein were used for the immunoprecipitation. Immunoprecipitation was performed as described above, and beads washed four times with lysis buffer. Samples were analyzed by SDS-PAGE and immunoblotting.

PI 4-Kinase Activity Assay

PI 4-kinase activity was measured essentially as described previously (Flanagan and Thorner, 1992; Walch-Solimena and Novick, 1999). Immunoprecipitations from soluble and membrane fractions were performed as described above. Immunocomplexes were washed, resuspended in PI-kinase buffer (50 mM Tris-HCl, 10 mM $MgCl_2$, and 0.25% Triton X-100), and aliquots were used for control Western blots and phosphoinositide analysis by thin TLC. Quantification of radioactive PI(4)P was performed by autoradiography of TLC plates by using the PhosphorImager BAS-1800II (Fuji, Tokyo, Japan).

Phosphorylation-dependent Gel Shift of Pik1p

Yeast cultures were grown to mid-log phase at 25°C, and if indicated, shifted to 37°C for 30 min. Cells were washed with ice-cold PBS, and the cultures were resuspended in lysis buffer (50 mM Tris-HCl, 1 mM EDTA, 150 mM NaCl, 1 mM PMSF, and Complete) with or without phosphatase inhibitors (25 mM NaF and 100 μM Na_3VO_4). All samples were homogenized by bead beating, and lysates were cleared by centrifugation (5 min; 2500 × *g*). Seventy-five micrograms of total protein of the sample without phosphatase inhibitors was treated with 5000 U of λ-PPase (New England Biolabs, Ipswich, MA) at 30°C for 30 min. Equal protein amounts were analyzed by 10% SDS-PAGE (500:1, acrylamide:bisacrylamide ratio) and immunoblotting.

RESULTS

Pik1p Binds to the 14-3-3 Proteins Bmh1p and Bmh2p

Pik1p has been reported to be present in a protein complex isolated by the TAP proteomic approach in which Bmh2p has been used as the bait (Gavin *et al*., 2002). Besides Pik1p, the Bmh2p complex contained Bmh1p, the second 14-3-3 protein found in yeast, the neutral trehalase proteins Nth1/2p, the transcription regulator Rtg2p, and the serine/threonine protein kinase Fun31p (Gavin *et al*., 2002). Using a yeast two-hybrid approach, we confirmed the interaction between Pik1p (amino acids [aa] 2–1066) and Bmh2p (Figure 1A, middle). Pik1p did not interact with other components of the Bmh2p complex in this assay (data not shown). The Pik1p–Bmh2p interaction was 10 times weaker than the interaction of Pik1p with Frq1p (Figure 1B). This interaction was lost upon deletion of the C-terminal catalytic domain of Pik1p (aa 770-1066) (Figure 1A, left). Bmh1p, which is highly similar to Bmh2p, also bound Pik1p in the yeast two-hybrid assay (Figure 1, A and B).

To confirm the observed interaction in vitro, we next tested the association of 14-3-3 GST fusions with endogenous Pik1p in GST pull-down experiments. Full-length Bmh1p and a construct encompassing a region of ~97% identity between Bmh1p and Bmh2p (GST-Bmh1$^{1\text{-}198}$) interacted with Pik1p from yeast lysates (Figure 1C). We then asked whether the Pik1p interaction with 14-3-3 is direct. Full-length Pik1p was synthesized by in vitro transcription and translation in the presence of [^{35}S]methionine. Radiolabeled Pik1p was incubated with GST-Bmh1p or GST-Bmh2p. As shown in Figure 1D, either GST fusion protein was able to pull down Pik1p, suggesting a direct interaction between the tested partners.

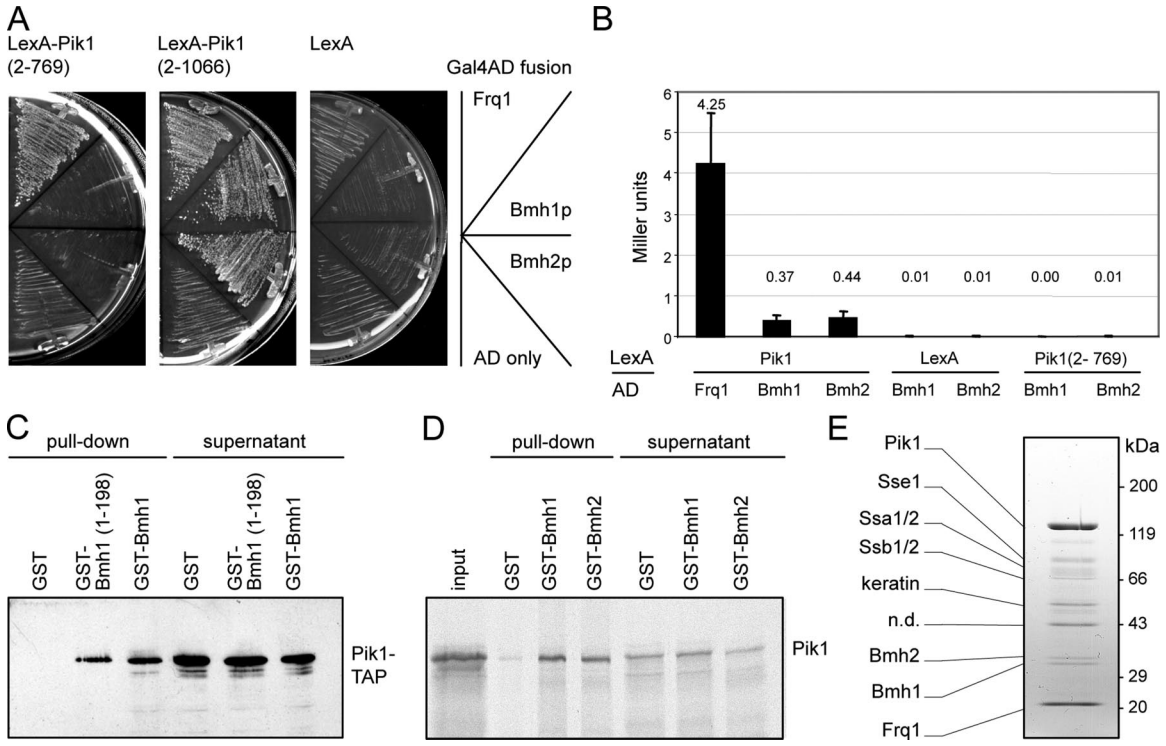

Figure 1. Interaction of Pik1p with the 14-3-3 proteins Bmh1/2p. (A) Pik1p and Bmh1/2p interact in the yeast two-hybrid system. Pik1p full-length (aa 2-1066; pMB138) and a C-terminal truncation (aa 2-769; pMB105) were expressed as LexA fusion proteins and targets as *GAL4* DNA activation domain fusions. Growth is shown on −His reporter plates. (B) Quantification of Pik1p-Bmh1p and Bmh2p interaction. β-Galactosidase activity was determined in the ONPG liquid culture assay (n = 5; mean ± SD). Frq1p was used as control. (C) GST-14-3-3 pull down of Pik1p from yeast lysates. GST-Bmh1p full length (pMB186) or truncated (aa 1-198; pMB241) fusion proteins were purified and incubated with a cleared yeast lysate (CSY513) in the presence of phosphatase inhibitors. Western blots were probed with anti-Pik1p polyclonal antibody. SDS-PAGE loads were normalized to equal amounts of GST-fusion proteins and Western blots probed with peroxidase anti-peroxidase (PAP) complex. (D) GST-14-3-3 pull down of in vitro-translated Pik1p. Pik1p was translated in vitro (pLD103) (TNT Quick-Coupled Transcription/Translation System) and incubated with GST-Bmh1p (pMB186) or GST-Bmh2p (pMB187) immobilized on glutathione-Sepharose. Radiolabeled Pik1p was detected by autoradiography. (E) Characterization of the Pik1p complex. TAP purification using a C-terminal Pik1p TAP tag (CSY370) was performed in the presence of phosphatase inhibitors, purified material was fractionated on a 4–16% gradient SDS-PAGE gel, and proteins were identified by MALDI-TOF and nanoES MS/MS. The analysis also identified common contaminants in TAP purification experiments: Sse1p, Ssa1/2p, Ssb1/2p, and human keratin. (n.d., not defined).

To test whether this interaction occurs in vivo, we performed a TAP experiment. The chromosomal copy of *PIK1* was fused to the TAP tag. The fusion protein of the essential PI 4-kinase was functional only when we inserted a six-amino acid linker (SGPGS) at the C terminus of Pik1p as suggested by normal growth of the resulting strain (data not shown). The identification of coisolated proteins by mass spectrometry revealed interaction of Pik1p, Bmh1p/Bmh2p, and Frq1p (Figure 1E), whereas other proteins represented common contaminants of the TAP procedure (Shevchenko *et al.*, 2002). We conclude that the Pik1p–14-3-3 complex occurs in vivo and includes both Bmh1p and Bmh2p, which often function as a heterodimer (Jones *et al.*, 1995).

Pik1p, Bmh1/2p, and Frq1p Occur in a Common Complex

The interaction of Pik1p with both Bmh1/2p and Frq1p opens the question whether these binding partners can occur in a common complex or bind in a mutually exclusive manner. We performed glycerol velocity gradient centrifugation to determine size and composition of Pik1p–14-3-3–containing protein complexes providing support for the existence of a heterotetrameric complex (Pik1p, Frq1p, and Bmh1/2p). As shown in Supplemental Figure 1, Pik1p and Frq1p were mainly present in fractions 3–10, with a peak in fractions 4–5 corresponding to ~230 kDa. The major pool of Bmh1p seems to be present in oligomeric complexes, because this protein is only weakly detectable in the monomer and dimer fractions 1–3. An antibody detecting both Bmh1p and Bmh2p revealed an identical behavior in the gradients, supporting involvement of heterodimers in the complex with Pik1p. This is in agreement with published data reporting that Bmh1/2p mainly occur as heterodimers (Chaudhri *et al.*, 2003). All four proteins together were found in a peak in fractions 5–7 that runs between 230 and 670 kDa, suggesting the presence of a heterotetrameric complex involving Pik1p, Frq1p, Bmh1p, and Bmh2p (Supplemental Figure 1).

For further confirmation of this hypothesis, we then isolated Frq1p–TAP-containing protein complexes using the TAP purification protocol (Figure 2). Western blotting of purified Frq1p–TAP complexes (Figure 2A) and mass spectrometry (Figure 2B and Supplemental Table 4) provided evidence for copurification of Bmh1/2p and thus for the presence of these proteins in a common protein complex.

BMH Function Interferes with the Late Secretory Pathway

The observed interaction of Bmh1p/Bmh2p with Pik1p prompted us to address a possible role of this complex in the regulation of secretion. Although we did not find synthetic

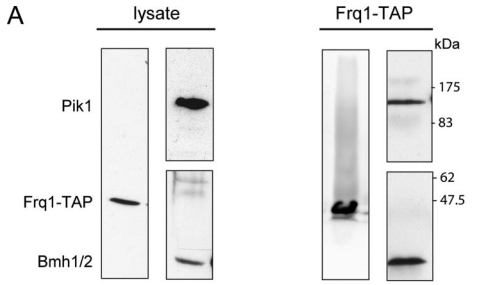

B MS results: Frq1p-TAP purification

Protein	Coverage	Description
Pik1p	56%	Phosphatidylinositol 4-kinase
Bmh1/2p	48%	14-3-3 proteins
Frq1p	47%	Frequenin-1

Figure 2. 14-3-3 proteins are present in a complex with Frq1p and Pik1p. (A) TAP purification using a C-terminal Frq1p TAP tag (Open Biosystems) was performed in the presence of phosphatase inhibitors and starting cell lysate, and purified material was analyzed by SDS-PAGE and Western blotting with anti-Pik1p, anti-Bmh1/2p, and PAP antibody. (B) Frq1p-TAP purified material was fractionated on a 4–16% gradient SDS-PAGE gel, and proteins were identified by nanoES MS/MS. For full list of identified proteins, see Supplemental Table 4.

genetic interaction of *bmh1*Δ or *bmh2*Δ with an allele of *pik1-101* impaired in catalytic activity (data not shown), we did observe enhancement of the growth defect of *pik1-101* by overproduction of Bmh proteins (2μ *BMH1* or *BMH2*) (Figure 3A). We further tested the effect of the overproduction of 14-3-3 in mutants along the secretory pathway (Supplementary Table 1). Synthetic enhancement of the growth defect by 14-3-3 overproduction was found in mutants of genes involved in Golgi vesicle formation (*arf1*Δ, *vps1*Δ, *ypt31*Δ *ypt32ts*, and *sec14-3*) and in mutants of genes required for TGN-to-plasma membrane transport (*sec1-1*, *sec2-41*, *sec2-59*, *sec3-2*, *sec4-8*, and *sec15-1*). This type of interaction was also found in mutants of cytoskeleton genes required for polarized transport of secretory vesicles (*act1-2* and *myo2-66*). No or a very weak genetic interaction was detected upon overexpression of *BMH1* or *BMH2* in mutants of genes in the general secretion gene *SEC19 (sec19-1*) or genes of endoplasmic reticulum-to-Golgi transport (*sec21-1*, *sec23-1*). Only the *N*-ethylmaleimide sensitive factor homologue *SEC18* (*sec18-1*) showed suppression of the growth phenotype upon 14-3-3 overexpression. In most cases, the synthetic genetic interaction of *BMH1/2* was found with mutant alleles of those *sec* mutants, which show synthetic sickness or lethality when combined with *pik1-101* (Walch-Solimena and Novick, 1999). These data suggested that both Pik1p and 14-3-3 might be involved in regulation of post-Golgi trafficking and that 14-3-3 overproduction counteracts Pik1p function.

To test more directly for a role of 14-3-3 proteins in membrane transport from the TGN together with Pik1p, we next used a visual assay for exocytosis. In *pik1-101* cells, surface transport of a GFP-tagged mutant version of the general amino acid permease Gap1p (Gap1*p-GFP lacking sites for ubiquitylation) is inhibited. This inhibition can be seen as dot-like accumulations, which could represent Golgi or endosomal structures (data not shown). Using this assay, we found an accumulation of Gap1*p-GFP compared with wild-type cells upon overexpression of *BMH2*, as we had detected in *pik1-101* (Figure 3, B and C). For a more quantitative evaluation of the Gap1*p-GFP transport defect, we measured Gap1p permease activity by uptake of [^{14}C]citrulline, an amino acid exclusively taken up through Gap1p (Roberg *et al*., 1997). In this assay, Gap1*p-GFP activity was fivefold reduced upon increased Bmh2p level (Figure 3D). Thus, in agreement with the described genetic interaction, Bmh2p overexpression seems to inhibit secretion, and likely negatively regulates Pik1p in this process as it shows similarities to loss of Pik1p activity. To understand how 14-3-3 proteins regulate Pik1p function, we first asked about the localization of the interaction.

Pik1p–14-3-3 Interaction Occurs in the Cytoplasm

Pik1p has been found at the TGN and in the nucleus (Walch-Solimena and Novick, 1999; Sciorra *et al*., 2005; Strahl *et al*., 2005). 14-3-3 proteins have a more widespread distribution. Fluorescence microscopy revealed a general cytoplasmic distribution of Bmh1p-myc with nuclear exclusion (Figure 4A). Bmh2p-myc was found in a punctate pattern throughout the entire cell. There was no obvious colocalization of Bmh proteins with Pik1p at the TGN (Figure 4A, insets). Because Pik1p immunofluorescence did not perfectly overlap with DAPI staining of DNA, we asked whether Pik1p could be concentrated in the nucleolus. As shown in Figure 4B, Pik1p colocalizes with a nucleolar marker (detected by monoclonal antibody [mAb] 2.3b; Yang *et al*., 1989). Due to the general cytoplasmic labeling for Bmh1p-myc and Bmh2p-myc, we could not exclude that there could be a pool of these proteins that localizes to this compartment. Therefore, we further investigated the subcellular localization by differential fractionation.

Pik1p-TAP and Bmh2p-myc were similarly distributed in fractions separated in a 13,000 $\times$ *g* and a 100,000 $\times$ *g* centrifugation step whereby both proteins were more abundant in the cytosol than in membrane fractions (Figure 4C). To determine whether Pik1p–14-3-3 interaction occurs in the cytosol or at the membrane, we performed immunoprecipitation experiments from either the supernatant or the pellet of the 100,000 $\times$ *g* centrifugation. Pik1p-myc coprecipitates Bmh1p-ha mainly from the cytosol, whereas little of the 14-3-3 protein binds to Pik1p-myc from the membrane pellet (Figure 4D). This suggests that Pik1p–14-3-3 interaction occurs mainly in the cytoplasm. We did not find significant differences in the PI 4-kinase activity of Pik1p-13myc immunoprecipitated from cytosol or membranes prepared as in Figure 4D (Figure 4E). Therefore, we hypothesized that 14-3-3 proteins might serve to regulate the localization of Pik1p, e.g., by formation of a Pik1p–14-3-3 complex in the cytoplasm, and this way might influence not only the availability of Pik1p at the TGN but also the amount of nuclear Pik1p.

Pik1p Is Primarily Nuclear upon Loss of 14-3-3 Function

To address a possible role of 14-3-3 in regulation of Pik1p distribution between cytosol and nucleus, we studied the localization of GFP-Pik1p in the background of *bmh* mutant alleles. Although GFP-Pik1p localized to the TGN and to the nucleus in wild-type cells (Figure 5, A–C), we observed an increased number of cells with nuclear Pik1p and decreased Pik1p levels at the TGN in *bmh1*Δ or *bmh1*Δ *bmh2ts* mutants at 25°C, an effect more pronounced at 37°C (Figure 5, A–C). Whole cell Pik1p levels were unchanged in *bmh* mutants at 25°C and in *bmh1*Δ at 37°C. There was a slight decrease at the restrictive temperature in the *bmh1*Δ *bmh2ts* double mutant (Supplemental Figure 2). Thus, the microscopy data indicate a true redistribution of Pik1p, suggesting that 14-3-3 interaction is required for maintenance of a pool of Pik1p in the cytoplasm and thus might make it accessible to the TGN. This idea is supported by our finding that in *bmh* mutants,

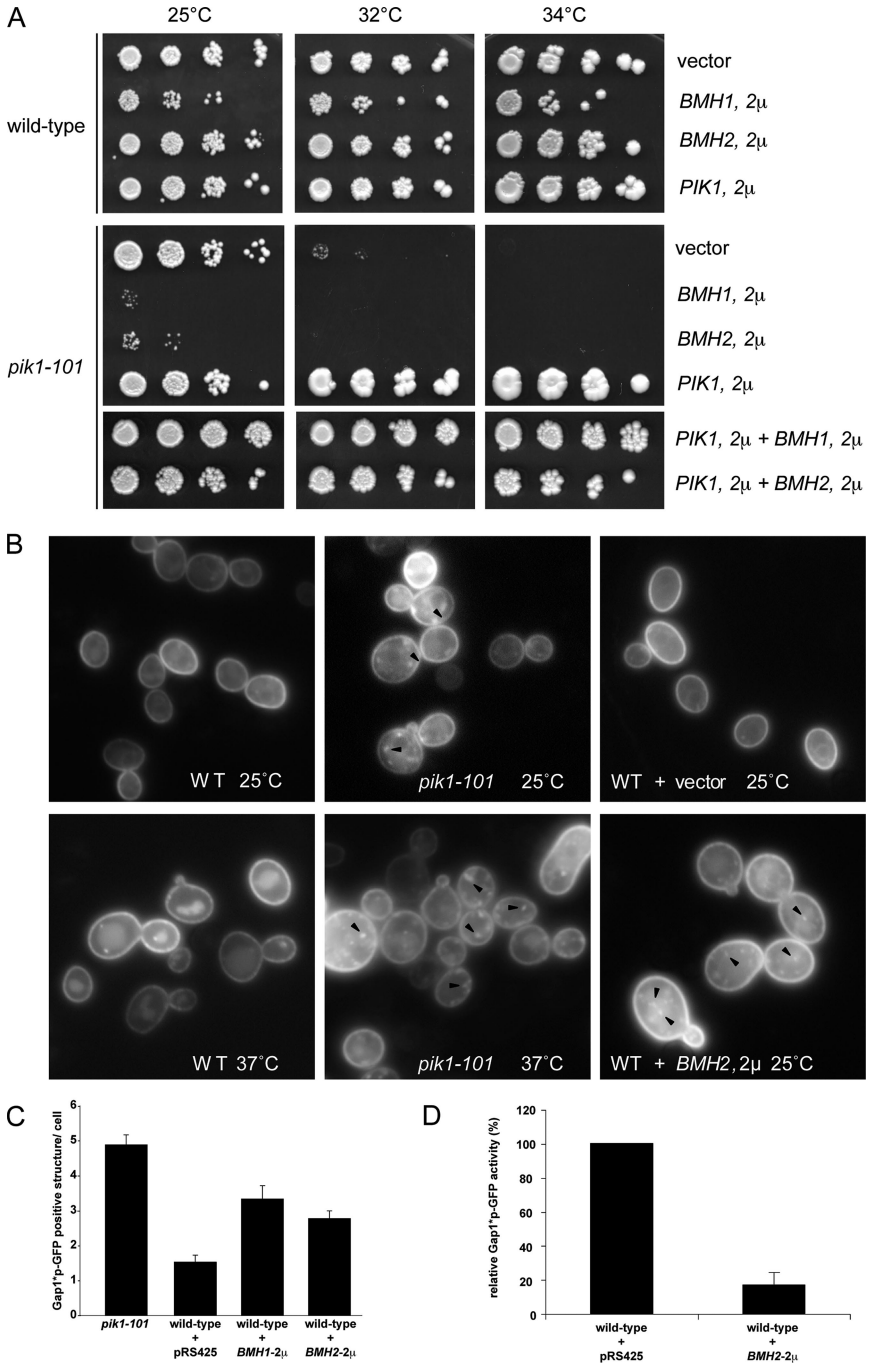

Figure 3. 14-3-3 overproduction interferes with late secretory pathway function. (A) Synthetic enhancement of *pik1-101* temperature-sensitive growth defect by high copy *BMH1/2*. The *pik1-101* mutant (CSY212) was transformed with 2μ *BMH1* (pMB180), 2μ *BMH2* (pMB181), 2μ *PIK1* (pCS8), or control vector (pRS426), and serial dilutions of cells were tested for growth at 25, 32, or 34°C. (B) Gap1*p-GFP surface transport is similarly impaired in *pik1-101* and wild-type cells overexpressing *BMH2* (pMB263). Wild-type (NY604) and *pik1-101* (YMB064) cells were transformed with Gap1*p-GFP (TPQ99). Cells were grown overnight at 25°C in SCRaf-URA and induced with 3% galactose for 3 h. The temperature shift was performed during the last hour of induction. Cells were analyzed by fluorescence microscopy. Gap1*p-GFP accumulation is indicated by arrowheads. (C) Gap1*p-GFP accumulating structures were counted for *pik1-101* (n = 68), wild-type (pRS425; n = 256), wild-type cells overexpressing *BMH1* (pMB262; n = 54) or overexpressing *BMH2* (pMB263; n = 243). Data are mean ± SEM. (D) Gap1*p-GFP surface activity is reduced in cells overexpressing *BMH2*. Cells were grown, and Gap1*p-GFP expression was induced as described in B. Gap1*p-GFP activity was determined by measuring the uptake of [^{14}C]citrulline. Data are mean ± SD (n = 3).

GFP-Pik1p still localizes to the Golgi; however, it does so with strongly decreased fluorescence intensity (Figure 5D and Supplemental Figure 3A). For quantification of the fluorescence intensity, we measured only structures smaller than 0.95 μm, thus excluding nuclei (Supplemental Figure 3B).

Pik1p–14-3-3 Interaction Involves Phosphorylation

The negative genetic interaction of 14-3-3 with Pik1p, the negative regulation of secretion by 14-3-3 overproduction, and the interaction between these proteins in the cytoplasm rather than at the TGN suggested that 14-3-3 might alter the availability of Pik1p for its function at the TGN. To further investigate the mechanisms underlying this regulation, we next asked how Pik1p–14-3-3 interaction itself is regulated. Because 14-3-3 proteins often bind to their targets through phosphorylated residues (Tzivion and Avruch, 2002; Yaffe, 2002; Dougherty and Morrison, 2004), we decided to investigate a possible phosphorylation dependence of the Pik1p–14-3-3 interaction.

GST pull-down experiments (GST-14-3-3) of genomically tagged Pik1p-TAP from yeast lysates were performed in the presence or absence of λ-PPase or phosphatase inhibitors. As shown in Figure 6A, Pik1p-TAP only bound to either GST-Bmh1p or GST-Bmh2p in the presence of phosphatase inhibitors, thus, Pik1p–14-3-3 interaction does require phos-

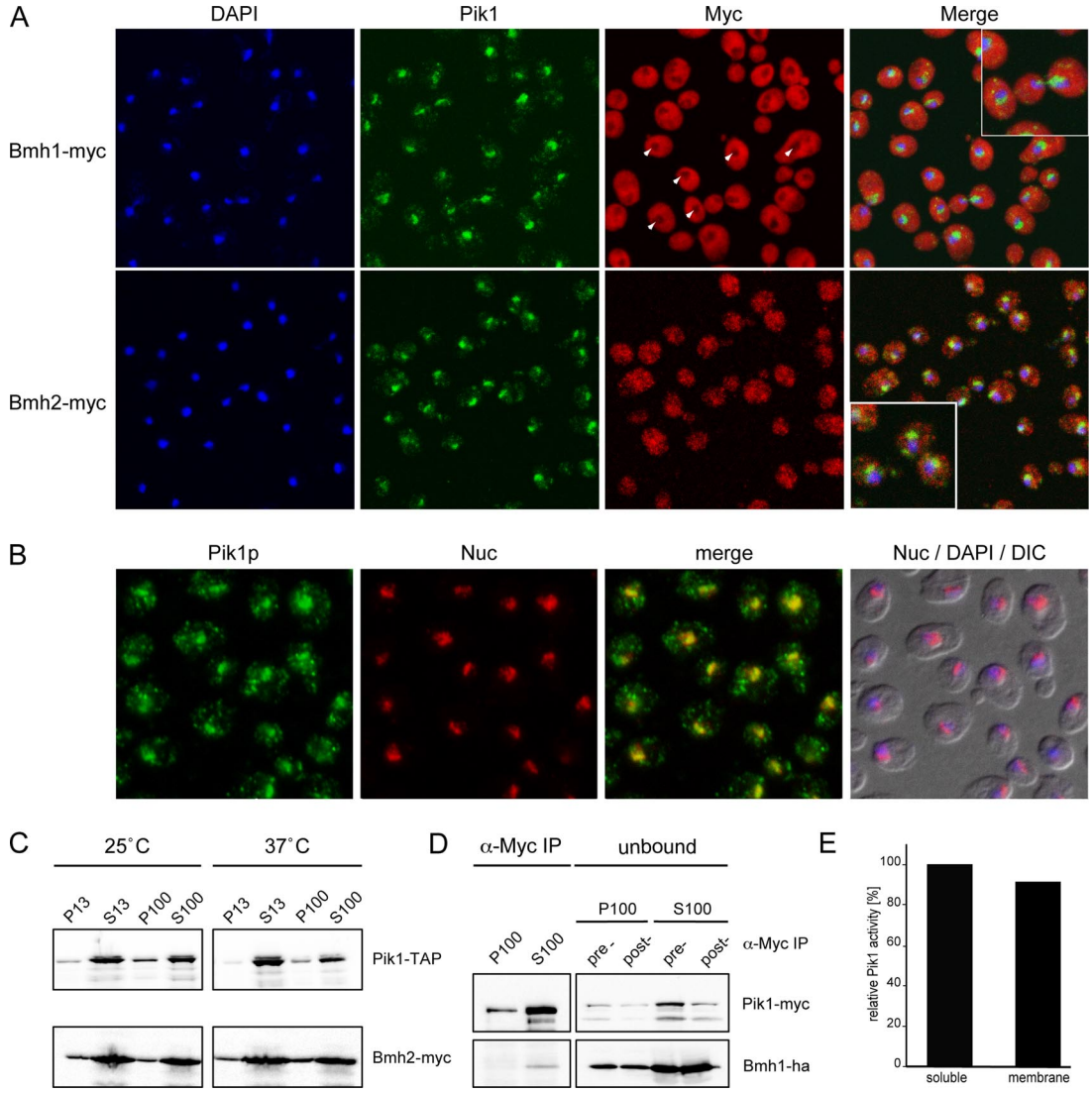

Figure 4. Localization of the Pik1p–14-3-3 interaction. (A) Subcellular localization of Pik1p and Bmh1/2p. *BMH1-13myc*– (YMB054) and *BMH2-13myc* (YMB058)–expressing cells were subjected to fixation, and Bmh proteins were labeled using anti-myc antibody (9E10) and Pik1p with anti-Pik1p antibody. DNA was stained with DAPI. Cells were viewed by fluorescence microscopy. (B) Pik1p is localized to the nucleolus. Wild-type cells (NY13) were labeled with anti-Pik1p antibody, mAb clone 2.3b for nucleoli, and DAPI. (C) Pik1p and Bmh1/2p distribution in subcellular fractions. Cells containing *PIK1-TAP* and *BMH2-13myc* (YMB119) were subjected to 13,000 × *g* and 100,000 × *g* centrifugation, and fractions examined by Western blotting. Pik1p-TAP was detected with PAP complex and Bmh1p-13myc or Bmh2p-13myc with anti-myc antibody (9E10). (D) Pik1p and 14-3-3 interact in the cytoplasm. Cells containing *PIK1-13myc* and *BMH1-3ha* (YMB148) were subjected to 100,000 × *g* centrifugation. After detergent lysis of the cytosolic or the membrane fraction, Pik1p-13myc was immunoprecipitated using anti-myc antibody (9E10). Coprecipitated Bmh1p-3ha was detected using anti-HA antibody (Y11). Loading controls represent 0.5% of the fractions. (E) PI 4-kinase activity of immunoprecipitated Pik1p from cytosol or membrane fractions prepared as described in D. Pik1p-13myc was precipitated with anti-myc antibody (9E10) and subjected to lipid-kinase assay by using phosphatidylinositol as substrate. Shown are results of two representative experiments. The amount of radioactive labeled PI(4)P was normalized to Pik1p-13myc protein levels.

phorylation. This finding is consistent with experiments in Figure 1, C and E, which were performed in the presence of phosphatase inhibitors. In vitro-translated Pik1p used for GST pull-down experiments shown in Figure 1D was partially phosphorylated (data not shown).

To determine which sites of Pik1p are phosphorylated, the protein was in-gel digested using different proteases (AspN, trypsin, and chymotrypsin), phosphorylated and unphosphorylated peptides were separated by titanium dioxide, and the phosphopeptides were analyzed by nanoLC tandem MS. Digestion with trypsin revealed mass peaks at m/z 1274.59, 1662.83, 981,43, and 1110.45, corresponding to the phosphorylated fragment ^{10}pSFDDTIELKK^{19}, ^{231}SSTPTpSPIDLIDPIK^{245}, ^{394}TNpSQPLSR^{401}, and ^{603}SDpSASTAVHR^{612}, respectively. The sites of phosphorylation within these fragments were unambiguously identified by tandem mass spectrometry (Table 1).

Two distinct 14-3-3 binding motifs have been described in the literature: RSXpS/TXP (mode 1; pS represents phosphorylated Ser/Thr and X any amino acid) and RXXXpS/TXP (mode 2) (Yaffe *et al*., 1997; Rittinger *et al*., 1999). Among the identified sites for phosphorylation, two (S396 and S605) are part of a predicted 14-3-3 target interaction motif according to Motif Scan (http://scansite.mit.edu). A third putative

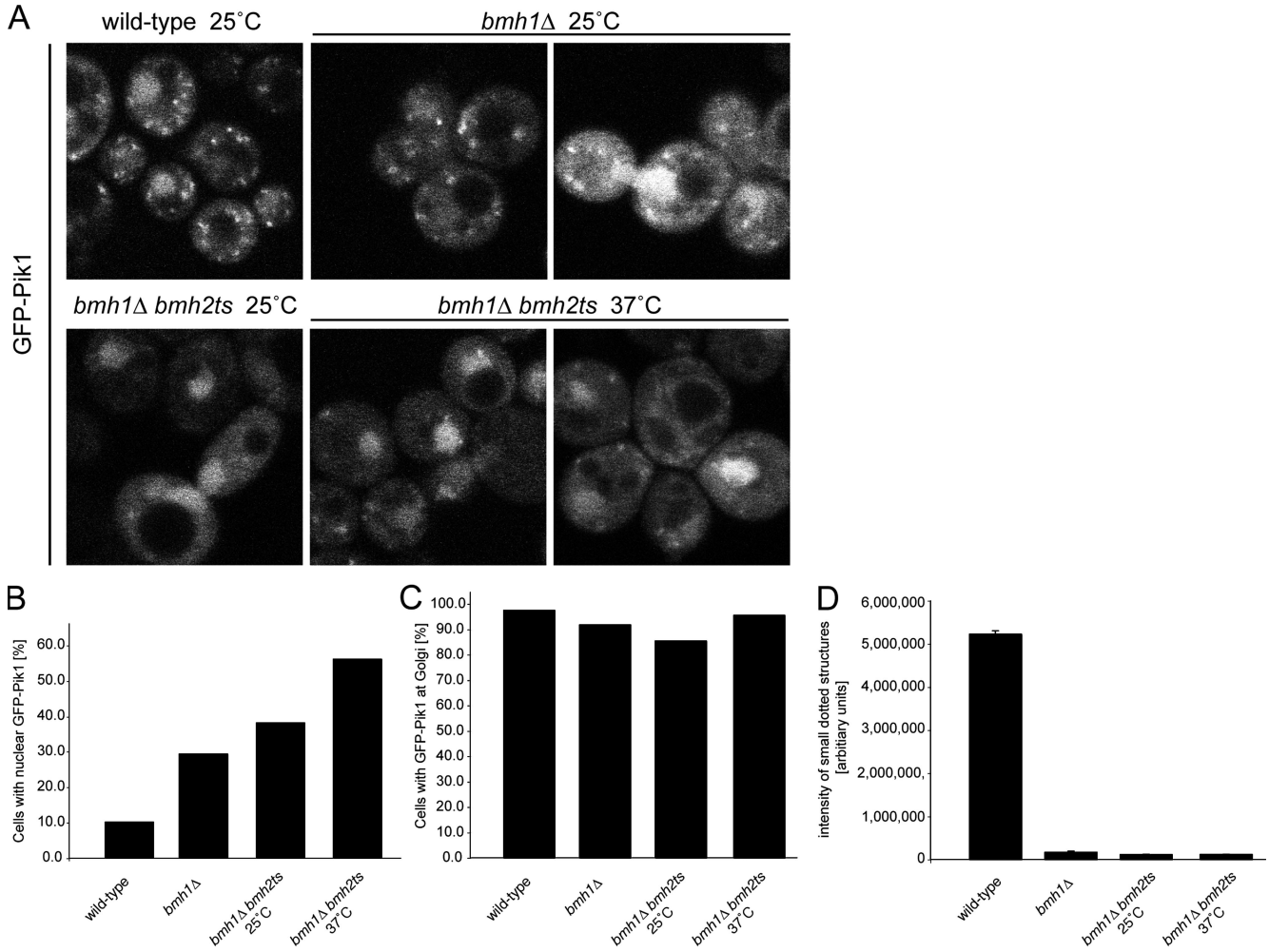

Figure 5. Functional 14-3-3 is required for normal Pik1p localization. Wild-type (NY1211), *bmh1*Δ (GG3001), and *bmh1*Δ *bmh2ts* (GG3000) mutant strains expressing *GFP-PIK1* from the endogenous promoter on a *CEN*-based plasmid were grown overnight, shifted to 37°C for 1 h when indicated, and visualized using a laser confocal microscope. (A) Laser confocal sections through the middle of representative cells in each treatment are shown. (B) Cells with nuclear GFP-Pik1p were counted (n = 80–90). (C) Cells with GFP-Pik1p at Golgi dots were counted (n = 80–90). (D) GFP-Pik1p fluorescence decreases in *bmh* mutants. Total intensity of small dotted structures (<0.95 μm in diameter) per cell for wild-type and mutant cells (mean ± SEM). For illustration of the quantification procedure, see Supplemental Figure 3.

14-3-3 binding motif was found at S780, a site that has not been identified by our mass spectrometry analysis. We generated mutants in these sites, tested for interaction of these mutated Pik1p proteins with Bmh1p and Bmh2p in the yeast two-hybrid assay and found that S396 is required for 14-3-3 interaction (Figure 6B). Together with the observed loss of interaction between Pik1p and 14-3-3 upon deletion of the catalytic domain of the PI 4-kinase (Figure 1A), we suggest that S396 is necessary but not sufficient for this interaction.

Pik1p Phosphorylation Correlates with Nucleocytoplasmic Relocalization

We next asked whether phosphorylation of Pik1p shows any correlation with its subcellular localization. We have previously described that Pik1p rapidly and reversibly relocalizes from the nucleus to the cytoplasm upon block of secretion, e.g., in a *sec6-4* mutant. The ASR occurs in *sec* mutants along the entire secretory pathway and also results in relocation of other nuclear proteins (Walch-Solimena and Novick, 1999; Nanduri and Tartakoff, 2001), probably by nuclear import inhibition (Nanduri *et al.*, 1999). We took advantage of the ASR and analyzed Pik1p phosphorylation in wild-type and *sec6-4* mutant cells after a 30-min shift to the restrictive temperature (Figure 6C). Under these conditions, a massive relocalization of nuclear Pik1p to the cytoplasm has been observed previously (Walch-Solimena and Novick, 1999).

To resolve the phosphorylated and nonphosphorylated form of Pik1p by SDS-PAGE, we empirically determined an acrylamide:bisacrylamide ratio of 500:1 as the best composition. On ASR in *sec6-4*, we detected a shift of Pik1p to a higher molecular weight form in lysates from *sec6-4* cells at the restrictive temperature compared with wild type. This shift was reversed upon treatment with λ-PPase, indicating that the higher molecular weight form is phosphorylated (Figure 6C). Together, the increase in phosphorylation and shuttling out of the nucleus of Pik1p during the ASR suggested that this modification might play a role in regulation of Pik1p distribution.

To test this further, we investigated the phosphorylation status of Pik1p in a mutant version of the protein showing a localization defect on its own. For this, we focused on the N-terminal regulatory domain of Pik1p, and we generated

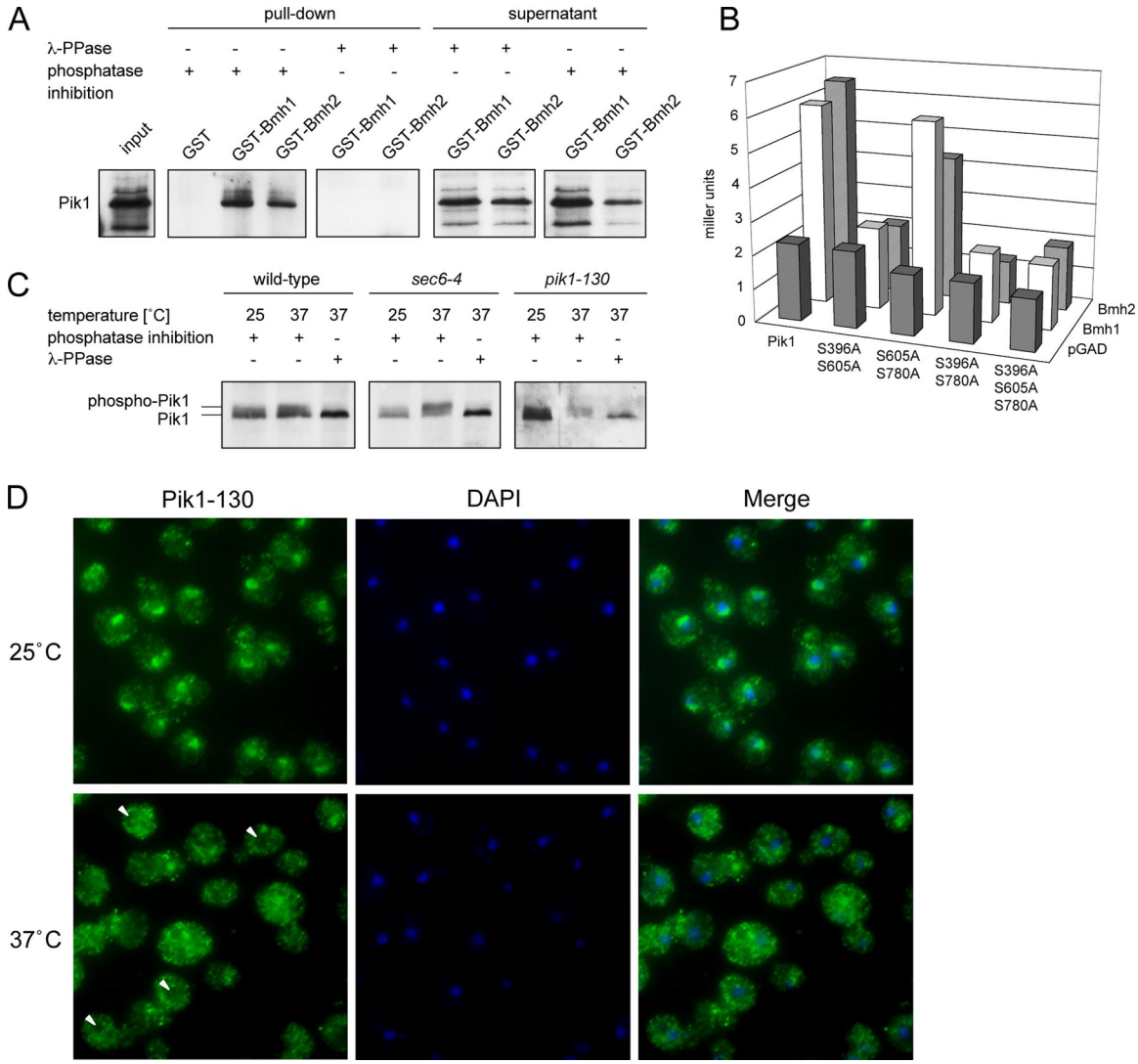

Figure 6. Pik1p interaction with 14-3-3 and localization is regulated by phosphorylation. (A) Pik1p binding to 14-3-3 requires phosphorylation. Extracts from cells containing Pik1p-TAP (CSY513) were either treated with λ-PPase or with phosphatase inhibitors followed by incubation with GST alone, GST-Bmh1p, or GST-Bmh2p immobilized on glutathione-Sepharose. Immunoblot analysis was with PAP complex. The input represents 5% of lysate. (B) Liquid β-galactosidase assay and yeast two-hybrid interactions of Pik1p phospho-mutants (*pik1-145* to *148*, pMB365-368, respectively) with Bmh1p (pMB116) and Bmh2p (pMB125) were quantified. Interaction between Pik1p (pMB138) and Bmh1p or Bmh2p serves as positive control, and interactions with pGADT7 as negative control. Values were from nine independent experiments. (C) Pik1p phosphorylation upon nucleocytoplasmic relocation. Wild-type (NY1211), *sec6-4* (NY778) and *pik1-130* (YMB087) cells were grown at 25°C, incubated for 30 min at 25 or 37°C as indicated, and lysed in the presence or absence of phosphatase inhibitors. Lysates without phosphatase inhibitors were incubated with λ-PPase. Samples were analyzed by SDS-PAGE (acrylamide: bisacrylamide ratio, 500:1) to resolve phosphorylated and nonphosphorylated Pik1p and immunoblotting with anti-Pik1p antibody. (D) The *pik1-130* mutant cells lack nuclear localization at the restrictive temperature. Cells carrying the *pik1-130* mutation (YMB087) were processed for immunofluorescence microscopy by using anti-Pik1p antibody and DAPI after incubation for 60 min at 25 or 37°C as indicated. Arrowheads indicate nuclear exclusion of Pik1-130p.

Table 1. Phosphorylation sites of Pik1p

Peptide sequence	Position (amino acids)	Phosphorylation at
pSFDDTIELKK	10–19	Ser10
SSTPTpSPIDLIDPIK	231–245	Ser236
TNpSQPLSR	394–401	Ser396
SDpSASTAHVR	603–612	Ser605

To identify the sites of phosphorylation, Pik1p was isolated by TAP purification from a strain expressing *PIK1-TAP*. After in-gel digestion with trypsin, the phosphorylated sequences were identified using a nanoLC ESI MS/MS.

temperature-sensitive *pik1* mutant alleles by error-prone PCR. Among the mutants we identified a new allele, *pik1-130*, which had a defect in nuclear but not the cytoplasmic punctate labeling for Pik1p (Figure 6D). Like Pik1p in Figure 4B, at the permissive temperature, mutant Pik1-130p localized immediately adjacent to DAPI, suggesting nucleolar localization (Figure 6D). At the restrictive temperature, when Pik1-130p no longer is nuclear, the protein was in part shifted to a higher molecular weight, phosphorylated form (Figure 6C) that could be detected even though the stability of the mutant protein was decreased. We con-

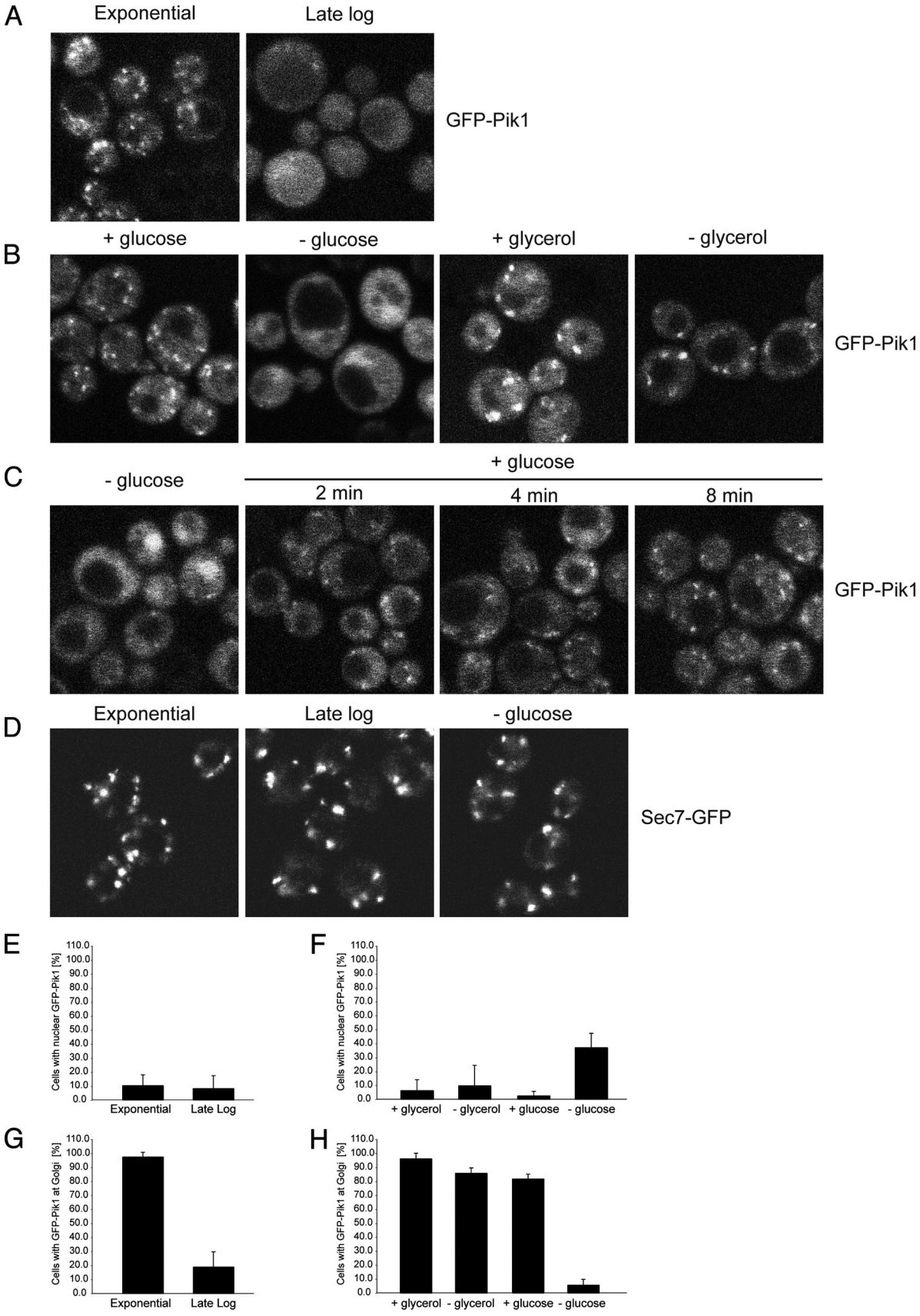

Figure 7. Pik1p relocalizes from the TGN to the cytoplasm and nucleus under growth-limiting conditions. (A) Pik1p is lost from the TGN in late log phase. Cells (NY1211) expressing *GFP-PIK1* from the endogenous promoter on a *CEN*-based plasmid were observed by laser

clude that the distribution of Pik1p correlates with its phosphorylation status. Together with the finding that Pik1p-14-3-3 interaction occurs in the cytoplasm and requires phosphorylation, we propose a model in which 14-3-3 proteins modulate nucleocytoplasmic shuttling of Pik1p. What could be the physiological significance of such a shuttling mechanism?

Pik1p Relocates from the TGN to the Nucleus under Conditions of Nutrient Limitation

We have shown that Pik1p redistributes from the nucleus to the cytosol during the ASR (Walch-Solimena and Novick, 1999), a condition where a rapid adjustment of the protein synthesis machinery occurs in response to a block in the secretory pathway (Mizuta and Warner, 1994; Nanduri and Tartakoff, 2001). Therefore, we asked whether a change in localization of Pik1p could also be observed under different growth conditions. For this, we observed GFP–Pik1p localization first in either early or late log phase growth. In early log phase cultures, only a small percentage of cells (9.0 ± 9.1%) showed nuclear GFP-Pik1p (Figure 7, A and E). Instead, all cells exhibited GFP-Pik1p labeling at the TGN (Figure 7, A and G). There was no obvious change in localization during the cell cycle (as judged by the size of the bud, data not shown). In late log phase, GFP-Pik1p became mostly cytoplasmic (Figure 7, A and G) without major change in nuclear (8.1 ± 9.1%) labeling (Figure 7, A and E). The TGN integrity was unchanged under these conditions since labeling with the TGN marker Sec7p-GFP was unaffected in late log phase cells (Figure 7D).

The change in Pik1p localization in response to growth prompted us to investigate the behavior of GFP-Pik1p in log phase cells under conditions of nutrient deprivation. In the absence of glucose, a strong increase in the nuclear labeling for GFP-Pik1p (37.1 ± 10.2%) and a concomitant loss of the lipid kinase from TGN membranes was observed (Figure 7, B, F, and H). Similar results were obtained for deprivation of raffinose or galactose (Supplemental Figure 4). No such effect was observed upon depletion of the nonfermentable carbon source glycerol (Figure 7, B, F, and H) or nitrogen starvation (data not shown), suggesting that only deprivation of fermentable carbon sources results in signaling that changes intracellular distribution of Pik1p. The TGN integrity was not disturbed under the nutrient deprivation conditions used as we observed normal labeling with Sec7p-GFP (Figure 7D). Also, ultrastructural analysis of glucose-deprived cells did not reveal any abnormal accumulation of the TGN (data not shown).

The relocalization of Pik1p from the TGN to the nucleus might represent a mechanism by which cells can quickly adjust both PI(4)P production and vesicle formation from the late Golgi to growth conditions. If such a signaling pathway existed, one would expect rapid restoration of the TGN localization of Pik1p if the appropriate carbon source (glucose, galactose or raffinose) is added back to the cells. As shown in Figure 7C, we did observe such a restoration of TGN localization of Pik1p within minutes after glucose addition. We obtained similar results using galactose (Supplemental Figure 5).

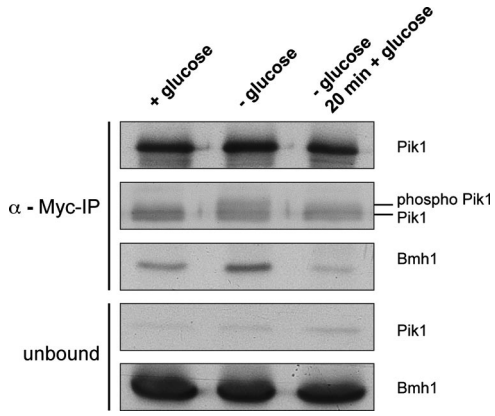

Figure 8. Relocation of Pik1p from the TGN to the cytoplasm is mediated by Pik1p phosphorylation and 14-3-3 binding. Early log phase cultures (YMB148) were depleted of glucose for 45 min. If indicated, glucose was added back to a final concentration of 2%. Pik1p-13myc was immunoprecipitated using anti-myc antibody (9E10). Coprecipitated Bmh1p-3ha was detected using anti-HA antibody (Y11). Samples were analyzed by SDS-PAGE (acrylamide: bisacrylamide ratio, 500:1) to resolve phosphorylated and nonphosphorylated Pik1p and immunoblotting with anti-myc antibody (9E10).

Pik1p Relocation under Nutrient Deprivation Involves Phosphorylation and 14-3-3 Binding

We next asked whether the observed relocation of Pik1p from the TGN to the cytoplasm and into the nucleus during nutrient deprivation might be mediated by Pik1p phosphorylation and 14-3-3 binding. For this, we performed a glucose deprivation experiment as shown in Figure 7, but this time we lysed cells after 45 min without glucose and 20 min after glucose readdition. As shown in Figure 8, more phosphorylated Pik1p was recovered after glucose deprivation than in control cells or after glucose readdition. Also, glucose deprivation resulted in an increase of Bmh1p in complex with Pik1p (Figure 8). Phosphorylation and 14-3-3 complex formation thus correlates with the observed loss of Pik1p from the TGN that results in relocation to the cytoplasm and to the nucleus.

We next investigated the role of Pik1p-14-3-3 interaction in the relocalization of Pik1p from the TGN to the nucleus. We observed that in cells co-overexpressing *BMH1* and *BMH2*, but not either gene alone, GFP-Pik1p no longer accumulated in the nucleus (Figure 9, A and B). TGN localization was unchanged compared with control cells both in the presence or absence of glucose (Figure 9, A and C). Thus, 14-3-3 levels seem to determine the amount of Pik1p kept in the cytoplasm after it has been released from the TGN. The Pik1p–14-3-3 complex might need to dissociate to allow for nuclear accumulation of Pik1p, because loss of 14-3-3 function results in increased nuclear accumulation (Figure 5). Together, these data suggest that nucleocytoplasmic shuttling of Pik1p is directly regulated by 14-3-3 interaction.

Figure 7. (cont). confocal microscopy. (B) Depletion of fermentable carbon sources results in shuttling of Pik1p from the TGN to the nucleus. Early log phase cultures (NY1211) were either depleted of glucose or glycerol for 45 min. (C) Relocalization of Pik1p from the TGN to the nucleus is reversed upon readdition of glucose. Cultures (NY1211) were depleted of glucose as described in B. After indicated times, glucose was added back to a final concentration of 2%. (D) The TGN marked by Sec7p-GFP is present in early log phase, late log phase, and glucose-depleted cells (YGY84). Cultures were treated as described in A or B. (E and F) Percentage of cells with nuclear GFP-Pik1p in A or B. (G and H) Percentage of cells with Golgi GFP-Pik1p in A or B. Values are mean ± SD (n = 100).

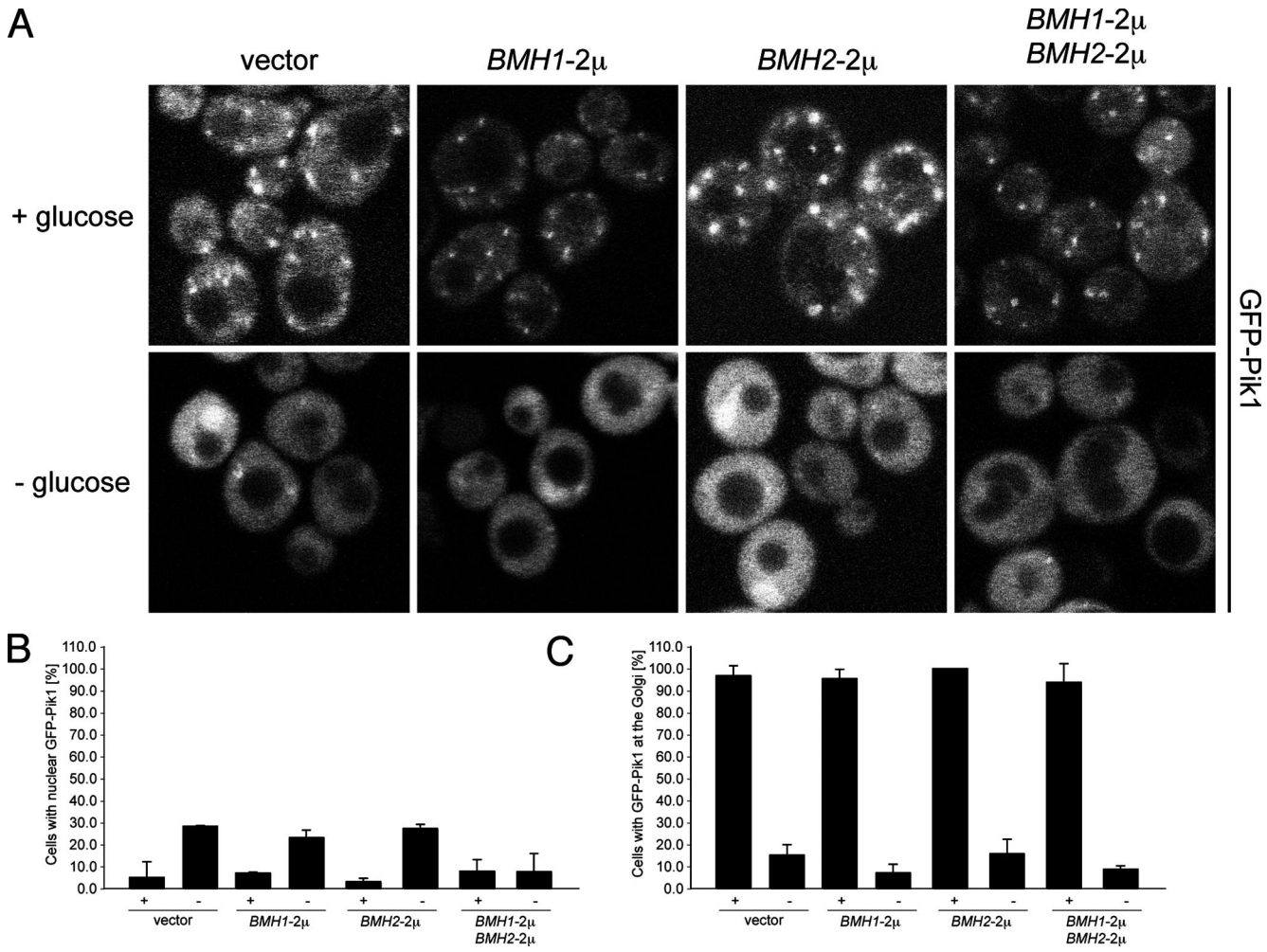

Figure 9. Co-overexpression of *BMH1* and *BMH2* prevents relocation of Pik1p to the nucleus upon glucose deprivation. (A) Early log phase cultures of cells (NY1211) expressing *GFP-PIK1* from the endogenous promoter on a *CEN*-based plasmid, and *BMH1* (pMB180), *BMH2* (pMB263), or *BMH1* and *BMH2* on a 2μ-based plasmid were depleted of glucose for 45 min. Cells were observed by confocal microscopy. (B and C) Number of cells with nuclear GFP-Pik1p (A) and with GFP-Pik1p at the Golgi (C) were plotted (mean ± SD).

Role of S396 Phosphorylation in Control of Cellular Pik1p Pools

To directly address the role of S396 phosphorylation in this process, we generated S396A and a corresponding phosphomimicking mutation S396D. GFP-Pik1^{S396A} or GFP-Pik1^{S396D}, like wild-type GFP-Pik1p, localized to the Golgi in the presence of glucose and they were lost from this compartment upon glucose deprivation (Figure 10, A and C). The GFP-Pik1^{S396A} protein was more nuclear in full media, and it accumulated approximately threefold more than wild type when glucose was removed (Figure 10, A and B). GFP-Pik1^{S396D} did behave like wild-type GFP-Pik1p with glucose, but it also accumulated more in the nucleus in the absence of glucose. Thus, S396 phosphorylation (and by extension 14-3-3 interaction) does not directly regulate Golgi association, but it does affect nucleocytoplasmic shuttling. The increased GFP-Pik1^{S396D} nuclear accumulation upon glucose deprivation might indicate that reversibility of phosphorylation is needed for the shuttling process (e.g., for nuclear exit).

We also measured PI 4-kinase activity of immunoprecipitated GFP-Pik1p compared with GFP-Pik1^{S396A} or GFP-Pik1^{S396D}, and we found no significant differences when equal amounts of immunoprecipitated GFP-Pik1 proteins were used for the assay (Figure 10, D and E). Thus, this phosphorylation (and 14-3-3 interaction) does not have a direct effect on the enzymatic activity of the lipid kinase.

We further took advantage of the S396 mutants to ask whether phosphorylation at this site regulates Pik1p–Frq1p interaction. In the yeast two-hybrid assay, we found no differences in the interaction of mutant versus wild-type Pik1p (Supplemental Figure 6). Together with our velocity gradient (Supplemental Figure 1) and Frq1p–TAP experiments (Figure 2), this suggests that S396 phosphorylation and 14-3-3 interaction do not function to regulate the Pik1p–Frq1p complex.

We have already shown that *BMH* overexpression can interfere with trafficking (Figure 3) and with nucleocytoplasmic shuttling (Figure 9). To investigate more directly the role of Pik1–14-3-3 interaction through phosphorylated S396 and trafficking, we measured endogenous Gap1p permease activity with the [^{14}C]citrulline uptake assay in yeast strains carrying *pik1*^{S396A} or *pik1*^{S396D}, respectively, as the only *PIK1* copy of the cell compared with cells carrying *PIK1* on the same plasmid (Supplemental Figure 7). We found a decrease in surface transport for S396A. These data further support the hypothesis that regulated nucleocytoplasmic shuttling and Pik1p function during trafficking are closely connected.

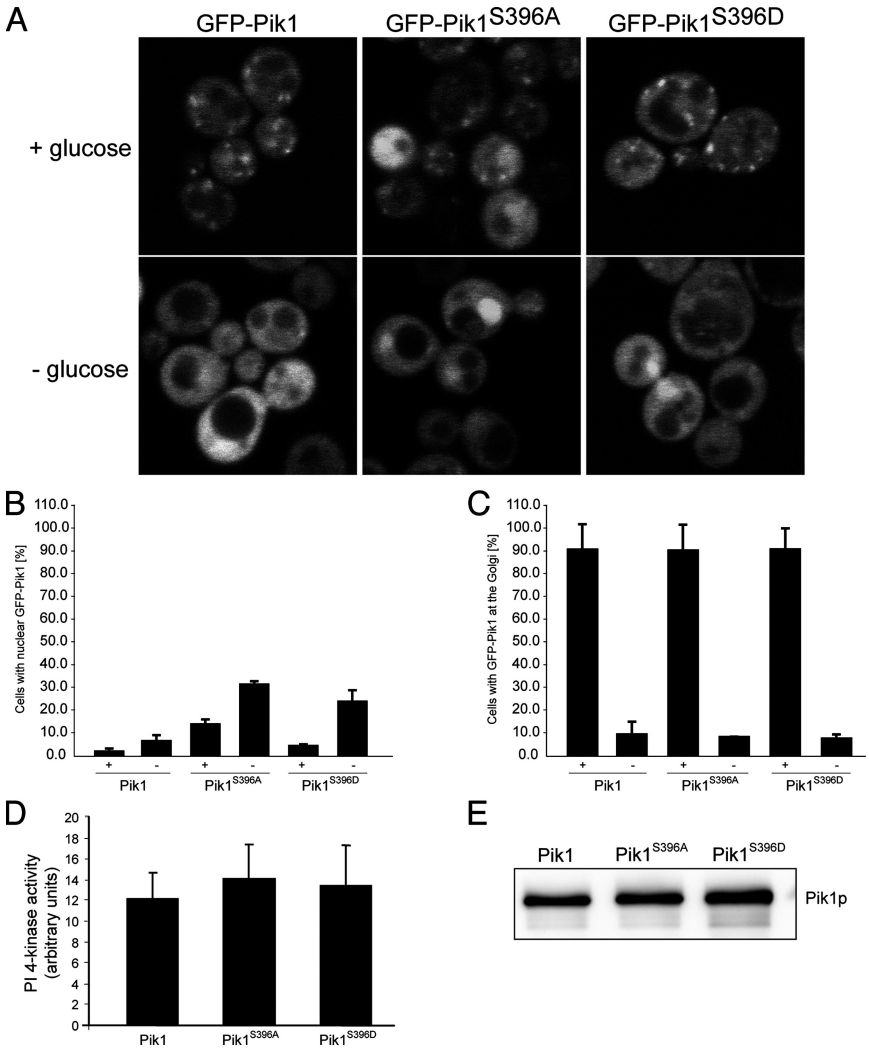

Figure 10. Pik1p phosphorylation site mutations affect nucleocytoplasmic shuttling but not Golgi association. (A) Cells (YMB003 containing pMB384) expressing *GFP-PIK1 (pMB422), GFP-PIK1(S396A) (pMB423),* or *GFP-PIK1(S396D) (pMB424*) from the *ADH* promoter on a *CEN*-based plasmid were observed by laser confocal microscopy. Depletion of glucose was performed as in Figure 7. (B) Percentage of cells with nuclear GFP-Pik1p. (C) Percentage of cells with Golgi GFP-Pik1p. Values are mean ± SD (n = 100). Similar results were obtained in absence of pMB384. (D) PI 4-kinase activity of S396 phosphorylation site mutants GFP-Pik1p, GFP-Pik1p^{S396A}, and GFP-Pik1p^{S396D}. GFP-Pik1p was precipitated with polyclonal anti-GFP antibody and subjected to lipid-kinase assay by using phosphatidylinositol as substrate. Results are from two representative experiments (mean ± SEM). (E) Representative immunoblot (monoclonal anti-GFP antibody) of immunoprecipitated GFP-Pik1p, GFP-Pik1p^{S396A}, and GFP-Pik1p^{S396D} for experiment (D).

DISCUSSION

Regulated Localization of PI-metabolizing Enzymes to Control Traffic

Our data suggest that the Golgi PI 4-kinase Pik1p is at least in part controlled by regulated localization. Previous studies reported that this enzyme localizes to the TGN and the nucleus (Garcia-Bustos *et al*., 1994; Walch-Solimena and Novick, 1999; Sciorra *et al*., 2005; Strahl *et al*., 2005). A similar dual localization has been found for PI 4-kinase IIIβ (Godi *et al*., 1999; de Graaf *et al*., 2002). Pik1p shuttles constitutively between nucleus and cytoplasm (Strahl *et al*., 2005). We provide evidence that 14-3-3 proteins regulate nucleocytoplasmic shuttling of this enzyme.

Bmh1p and Bmh2p bind to Pik1p in vitro and in vivo depending on phosphorylation, a modification involved in 14-3-3 target binding (Tzivion and Avruch, 2002; Yaffe, 2002; Dougherty and Morrison, 2004). During the ASR, Pik1p rapidly relocates from the nucleus to the cytoplasm and undergoes a shift to the phosphorylated form, suggesting that Pik1p needs phosphorylation for cytoplasmic localization. Consistent with this model, we found an increase in phosphorylated Pik1p and Pik1p–14-3-3 complex during nutrient deprivation, when Pik1p is no longer TGN-bound but becomes cytoplasmic, before it accumulates in the nucleus. Membrane-associated Pik1p binds to 14-3-3 only to a small extent.

We were unable to disrupt Pik1p–14-3-3 complexes from cell lysates either with phosphatases or by competition with the R18 peptide, a peptide which competes with 14-3-3 interactors (Wang *et al*., 1999; data not shown), suggesting that dissociation of 14-3-3 from Pik1p is regulated and might precede dephosphorylation. This interaction might thus protect cytoplasmic Pik1p from dephosphorylation, possibly to offer phosphorylated Pik1p to the TGN. According to our data, membrane binding of Pik1p and Pik1p–Frq1p interaction occurs by a mechanism not requiring 14-3-3 function (see model in Figure 11). Instead, Pik1p binding to the Golgi does require Frq1p (Strahl *et al*., 2005). Such a model would be consistent with our finding that 14-3-3 overproduction interferes with function of the late secretory pathway.

What is the function of cytoplasmic Pik1p–14-3-3 complexes? We have developed a kinetic model for Pik1p localization (see Supplemental Material) in which, in agreement with our microscopic observations, release of Pik1p from the Golgi results in an increase of both cytoplasmic and nuclear Pik1p. Our biochemical data provide some evidence for an increase of the cytosolic pool, because we find an increase in Pik1p–14-3-3 complex, probably caused by increased cytosolic concentration of Pik1p. The 14-3-3 interaction appar-

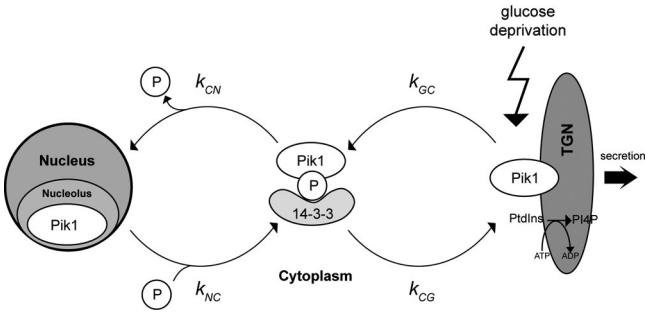

Figure 11. Model of the role of 14-3-3 interaction in the regulation of cellular Pik1p pools. A cytoplasmic Pik1p–14-3-3 complex maintains a pool of Pik1p that can be recruited to the TGN, where Pik1p binds to the membrane through the action of Frq1p and produces PI(4)P. Cytoplasmic Pik1p is protected from dephosphorylation and nuclear import through the action of 14-3-3. Glucose deprivation releases Golgi Pik1p, increases Pik1p–14-3-3 complex formation, and, possibly due to an effective increase in Pik1p concentration, increases also the nuclear pool. This regulation might provide a very rapid mode of adjustment of PI(4)P levels and thus transport capacity of the Golgi to coordinate nutrient signaling with growth. The *k*-values represent hypothetical reaction constants (see *Discussion* and Supplemental Material).

ently determines how much of Pik1p can remain cytoplasmic and thus ready for Golgi recruitment. Both S396 phosphorylation and 14-3-3 protein levels can regulate availability of Pik1p, because we see an effect of these parameters on the Gap1p permease activity at the plasma membrane.

An important role of phosphorylation in PI 4-kinase regulation was also described for PI 4-kinase IIIβ (Hausser *et al*., 2005). Protein kinase D, which mediates fission of transport carriers from the TGN (Liljedahl *et al*., 2001), phosphorylates PI 4-kinase IIIβ at a site (S294) within a region of homology between class III PI 4-kinases (Hausser *et al*., 2005). Interestingly, one of the phospho-serines identified in our study (S396) is located within this conserved region and the phosphorylation site S294 of PI 4-kinase IIIβ also lies within a 14-3-3 consensus binding motif (Hausser *et al*., 2006). Even though phosphorylated PI 4-kinase IIIβ localizes to the TGN, phosphorylation (in position S294) is not required for this localization but rather for enzymatic activity (Hausser *et al*., 2005; Szivak *et al*., 2006). We did not find differences in Pik1p activity immunoprecipitated from cytosol or membrane fractions or in mutants of S396, suggesting that control of Pik1p enzymatic activity is not a major function of S396 phosphorylation and binding of 14-3-3 proteins.

PI 4-kinase IIIβ accumulated in the nucleus of cells treated with leptomycin B (de Graaf *et al*., 2002). However, the mammalian PI 4-kinase was not detected in the nucleus under steady-state conditions, making it difficult to compare the nucleocytoplasmic shuttling process with the yeast system. Therefore, it will be of interest to address whether control of nucleocytoplasmic shuttling of type III PI 4-kinases by 14-3-3 proteins is conserved.

Regulation of the localization of enzymes of PI metabolism has been documented in other studies, e.g., for the PI(4)P 5-kinase Mss4p (Audhya and Emr, 2003) and the lipid phosphatase Sac1p (Faulhammer *et al*., 2005; Faulhammer *et al*., 2007). Together with our data showing nucleocytoplasmic shuttling of Pik1p, we propose that relocation of PI-metabolizing enzymes between different compartments might be a general mechanism for the rapid adjustment of PI levels on organelles. Our work revealed one mechanism by which such shuttling of a PI kinase might be controlled: formation of a complex with 14-3-3 proteins.

Do 14-3-3 Proteins Coordinate Golgi Function with Nutrient Signaling?

Use of a phosphorylation-dependent and 14-3-3–dependent mechanism for regulated subcellular distribution of Pik1p provides in addition to rapid and local control of PI(4)P production the possibility of coupling Pik1p function to signaling processes, which might need to be coordinated with membrane transport. We did indeed find that 14-3-3 proteins affect secretion, and that Pik1p–14-3-3 interaction mediates relocation of Pik1p in response to nutrient limitation. We propose that 14-3-3 proteins act as a gatekeeper for Golgi Pik1p through control of cytoplasmic Pik1p levels and nucleocytoplasmic shuttling.

14-3-3 proteins have previously been implicated in membrane transport regulation (Gelperin *et al*., 1995; Vasara *et al*., 2002) and cytoskeleton organization (Roth *et al*., 1999), but so far little is known about the targets of these proteins. We found here that overexpression of *BMH1* or *BMH2* was lethal in the actin mutant *act1-2* and a mutant of the myosin motor of secretory vesicles (*myo2-66*), together suggesting that 14-3-3 proteins, on their own or with Pik1p, could regulate the actin cytoskeleton. This regulation is likely to contribute to the effects of 14-3-3 on post-Golgi transport. Besides a defect in actin polarization, *bmh* and *pik1* mutants both exhibit defects in budding and cell wall integrity (Lottersberger *et al*., 2006; data not shown), which could be related to membrane transport but could also point toward additional roles of both proteins.

We found that phosphorylation of Pik1p and Pik1p–14-3-3 complex formation is subject to regulation both in the ASR and under nutrient deprivation conditions. Therefore, we propose that this interaction could be part of a signaling pathway that coordinates growth conditions with Golgi function. 14-3-3 proteins have been implicated in many cellular processes. In yeast, they participate in the Ras/mitogen-activated protein kinase cascade of pseudohyphal development (Roberts *et al*., 1997), the target of rapamycin (TOR) pathway (Gelperin *et al*., 1995; Bertram *et al*., 1998; Beck and Hall, 1999), the RAS–cAMP pathway (Gelperin *et al*., 1995), and possibly in the cell wall integrity pathway (Lottersberger *et al*., 2006). Because we found that deprivation of fermentable carbon sources results in rapid and reversible relocation of Pik1p and increased Pik1p–14-3-3 interaction, the TOR and the Ras pathways are possible candidates for upstream signaling. It will now be important to identify the kinases for Pik1p phosphorylation.

Is there a coordination of growth with secretion via PI(4)P signaling? Interestingly, we found Pik1p loss from the TGN under similar conditions that caused relocation of the lipid phosphatase Sac1p from the ER to the Golgi (Faulhammer *et al*., 2005, 2007). Because Pik1p generates PI(4)P and Sac1p dephosphorylates this lipid, the coordinated relocation of both enzymes would result in a drastic and rapid reduction of PI(4)P on the TGN membrane. This in turn would reduce PI(4)P-dependent membrane transport and coordinate SV production with growth conditions. Indeed, it has been reported that a fluorescent PI(4)P-binding PH domain no longer localized to the Golgi under conditions of glucose deprivation (Faulhammer *et al*., 2005) similar to the conditions used in our study. It is now of great interest whether this signaling pathway is conserved in vertebrates. Interestingly, Frq1p, a positive regulator of function of the fission yeast Pik1p homologue, participates in nutrient-regulated signaling pathways (Hamasaki-Katagiri *et al*., 2004).

The Golgi apparatus is not only a major hub for transport in the secretory pathway but also an important signaling platform. Further work on the role of the Pik1p–14-3-3 interaction will provide new insights of how membrane transport at the Golgi is coordinated with growth.

ACKNOWLEDGMENTS

We are indebted to Benjamin Glick (University of Chicago, Chicago, IL), Peter Novick (Yale University, New Haven, CT), Jeremy Thorner (University of California, Berkeley), and G. Paul H. van Heusden (Leiden University, the Netherlands), for sharing constructs and yeast strains. We are grateful to Assen Roguev and Daniel Schaft for advice with the TAP technique. For many helpful discussions and comments on the manuscript, we thank Wolfgang Zachariae, Bernard Hoflack, and Marcos Gonzales-Gaitan. This work was supported by the Max Planck Society.

REFERENCES

Ames, J. B., Hendricks, K. B., Strahl, T., Huttner, I. G., Hamasaki, N., and Thorner, J. (2000). Structure and calcium-binding properties of Frq1, a novel calcium sensor in the yeast *Saccharomyces cerevisiae*. Biochemistry *39*, 12149–12161.

Audhya, A., and Emr, S. D. (2003). Regulation of PI4,5P2 synthesis by nuclear-cytoplasmic shuttling of the Mss4 lipid kinase. EMBO J. *22*, 4223–4236.

Audhya, A., Foti, M., and Emr, S. D. (2000). Distinct roles for the yeast phosphatidylinositol 4-kinases, Stt4p and Pik1p, in secretion, cell growth, and organelle membrane dynamics. Mol. Biol. Cell *11*, 2673–2689.

Bauer, P. J., and Krause, E. (2005). Accessibility of cysteines in the native bovine rod cGMP-gated channel. Biochemistry *44*, 1624–1634.

Beck, T., and Hall, M. N. (1999). The TOR signalling pathway controls nuclear localization of nutrient-regulated transcription factors. Nature *402*, 689–692.

Bertram, P. G., Zeng, C., Thorson, J., Shaw, A. S., and Zheng, X. F. (1998). The 14-3-3 proteins positively regulate rapamycin-sensitive signaling. Curr. Biol. *8*, 1259–1267.

Brickley, K., Smith, M. J., Beck, M., and Stephenson, F. A. (2005). GRIF-1 and OIP106, members of a novel gene family of coiled-coil domain proteins: association in vivo and in vitro with kinesin. J. Biol. Chem. *280*, 14723–14732.

Chaudhri, M., Scarabel, M., and Aitken, A. (2003). Mammalian and yeast 14-3-3 isoforms form distinct patterns of dimers in vivo. Biochem. Biophys. Res. Commun. *300*, 679–685.

de Graaf, P., Klapisz, E. E., Schulz, T. K., Cremers, A. F., Verkleij, A. J., and van Bergen en Henegouwen, P. M. (2002). Nuclear localization of phosphatidylinositol 4-kinase beta. J. Cell Sci. *115*, 1769–1775.

Dougherty, M. K., and Morrison, D. K. (2004). Unlocking the code of 14-3-3. J. Cell Sci. *117*, 1875–1884.

Du, L. L., and Novick, P. (2001). Yeast rab GTPase-activating protein Gyp1p localizes to the Golgi apparatus and is a negative regulator of Ypt1p. Mol. Biol. Cell *12*, 1215–1226.

Faulhammer, F., Kanjilal-Kolar, S., Knodler, A., Lo, J., Lee, Y., Konrad, G., and Mayinger, P. (2007). Growth control of Golgi phosphoinositides by reciprocal localization of sac1 lipid phosphatase and pik1 4-kinase. Traffic *8*, 1554–1567.

Faulhammer, F., Konrad, G., Brankatschk, B., Tahirovic, S., Knodler, A., and Mayinger, P. (2005). Cell growth-dependent coordination of lipid signaling and glycosylation is mediated by interactions between Sac1p and Dpm1p. J. Cell Biol. *168*, 185–191.

Flanagan, C. A., and Thorner, J. (1992). Purification and characterization of a soluble phosphatidylinositol 4-kinase from the yeast *Saccharomyces cerevisiae*. J. Biol. Chem. *267*, 24117–24125.

Garcia–Bustos, J. F., Marini, F., Stevenson, I., Frei, C., and Hall, M. N. (1994). PIK1, an essential phosphatidylinositol 4-kinase associated with the yeast nucleus. EMBO J. *13*, 2352–2361.

Gavin, A. C. *et al*. (2002). Functional organization of the yeast proteome by systematic analysis of protein complexes. Nature *415*, 141–147.

Gelperin, D., Weigle, J., Nelson, K., Roseboom, P., Irie, K., Matsumoto, K., and Lemmon, S. (1995). 14-3-3 proteins: potential roles in vesicular transport and Ras signaling in *Saccharomyces cerevisiae*. Proc. Natl. Acad. Sci. USA *92*, 11539–11543.

Godi, A. *et al*. (2004). FAPPs control Golgi-to-cell-surface membrane traffic by binding to ARF and PtdIns(4)P. Nat. Cell Biol. *6*, 393–404.

Godi, A., Pertile, P., Meyers, R., Marra, P., Di Tullio, G., Iurisci, C., Luini, A., Corda, D., and De Matteis, M. A. (1999). ARF mediates recruitment of PtdIns-4-OH kinase-beta and stimulates synthesis of PtdIns(4,5)P2 on the Golgi complex. Nat. Cell Biol. *1*, 280–287.

Hama, H., Schnieders, E. A., Thorner, J., Takemoto, J. Y., and DeWald, D. B. (1999). Direct involvement of phosphatidylinositol 4-phosphate in secretion in the yeast *Saccharomyces cerevisiae*. J. Biol. Chem. *274*, 34294–34300.

Hamasaki-Katagiri, N., Molchanova, T., Takeda, K., and Ames, J. B. (2004). Fission yeast homolog of neuronal calcium sensor-1 (Ncs1p) regulates sporulation and confers calcium tolerance. J. Biol. Chem. *279*, 12744–12754.

Hausser, A., Link, G., Hoene, M., Russo, C., Selchow, O., and Pfizenmaier, K. (2006). Phospho-specific binding of 14-3-3 proteins to phosphatidylinositol 4-kinase III beta protects from dephosphorylation and stabilizes lipid kinase activity. J. Cell Sci. *119*, 3613–3621.

Hausser, A., Storz, P., Martens, S., Link, G., Toker, A., and Pfizenmaier, K. (2005). Protein kinase D regulates vesicular transport by phosphorylating and activating phosphatidylinositol-4 kinase IIIbeta at the Golgi complex. Nat. Cell Biol. *7*, 880–886.

Heldwein, E. E., Macia, E., Wang, J., Yin, H. L., Kirchhausen, T., and Harrison, S. C. (2004). Crystal structure of the clathrin adaptor protein 1 core. Proc. Natl. Acad. Sci. USA *101*, 14108–14113.

Hendricks, K. B., Wang, B. Q., Schnieders, E. A., and Thorner, J. (1999). Yeast homologue of neuronal frequenin is a regulator of phosphatidylinositol-4-OH kinase. Nat. Cell Biol. *1*, 234–241.

Jones, D. H., Ley, S., and Aitken, A. (1995). Isoforms of 14-3-3 protein can form homo- and heterodimers in vivo and in vitro: implications for function as adapter proteins. FEBS Lett. *368*, 55–58.

Liljedahl, M., Maeda, Y., Colanzi, A., Ayala, I., Van Lint, J., and Malhotra, V. (2001). Protein kinase D regulates the fission of cell surface destined transport carriers from the trans-Golgi network. Cell *104*, 409–420.

Longtine, M. S., McKenzie, A., 3rd, Demarini, D. J., Shah, N. G., Wach, A., Brachat, A., Philippsen, P., and Pringle, J. R. (1998). Additional modules for versatile and economical PCR-based gene deletion and modification in *Saccharomyces cerevisiae*. Yeast *14*, 953–961.

Lottersberger, F., Panza, A., Lucchini, G., Piatti, S., and Longhese, M. P. (2006). The *Saccharomyces cerevisiae* 14-3-3 proteins are required for the G1/S transition, actin cytoskeleton organization and cell wall integrity. Genetics *173*, 661–675.

Miller, J. (1972). Experiments in Molecular Genetics, Cold Spring Harbor, NY: Cold Spring Harbor Laboratory Press.

Mizuta, K., and Warner, J. R. (1994). Continued functioning of the secretory pathway is essential for ribosome synthesis. Mol. Cell. Biol. *14*, 2493–2502.

Muslin, A. J., and Xing, H. (2000). 14-3-3 proteins: regulation of subcellular localization by molecular interference. Cell Signal. *12*, 703–709.

Nanduri, J., Mitra, S., Andrei, C., Liu, Y., Yu, Y., Hitomi, M., and Tartakoff, A. M. (1999). An unexpected link between the secretory path and the organization of the nucleus. J. Biol. Chem. *274*, 33785–33789.

Nanduri, J., and Tartakoff, A. M. (2001). The arrest of secretion response in yeast: signaling from the secretory path to the nucleus via Wsc proteins and Pkc1p. Mol Cell *8*, 281–289.

Nigg, E. A. (1997). Nucleocytoplasmic transport: signals, mechanisms and regulation. Nature *386*, 779–787.

Pinkse, M. W., Uitto, P. M., Hilhorst, M. J., Ooms, B., and Heck, A. J. (2004). Selective isolation at the femtomole level of phosphopeptides from proteolytic digests using 2D-NanoLC-ESI-MS/MS and titanium oxide precolumns. Anal. Chem. *76*, 3935–3943.

Puig, O., Caspary, F., Rigaut, G., Rutz, B., Bouveret, E., Bragado-Nilsson, E., Wilm, M., and Seraphin, B. (2001). The tandem affinity purification (TAP) method: a general procedure of protein complex purification. Methods *24*, 218–229.

Rigaut, G., Shevchenko, A., Rutz, B., Wilm, M., Mann, M., and Seraphin, B. (1999). A generic protein purification method for protein complex characterization and proteome exploration. Nat. Biotechnol. *17*, 1030–1032.

Rink, J., Ghigo, E., Kalaidzidis, Y., and Zerial, M. (2005). Rab conversion as a mechanism of progression from early to late endosomes. Cell *122*, 735–749.

Rittinger, K., Budman, J., Xu, J., Volinia, S., Cantley, L. C., Smerdon, S. J., Gamblin, S. J., and Yaffe, M. B. (1999). Structural analysis of 14-3-3 phosphopeptide complexes identifies a dual role for the nuclear export signal of 14-3-3 in ligand binding. Mol Cell *4*, 153–166.

Roberg, K. J., Rowley, N., and Kaiser, C. A. (1997). Physiological regulation of membrane protein sorting late in the secretory pathway of *Saccharomyces cerevisiae*. J. Cell Biol. *137*, 1469–1482.

Roberts, R. L., Mosch, H. U., and Fink, G. R. (1997). 14-3-3 proteins are essential for RAS/MAPK cascade signaling during pseudohyphal development in *S. cerevisiae*. Cell *89*, 1055–1065.

Roth, D., Birkenfeld, J., and Betz, H. (1999). Dominant-negative alleles of 14-3-3 proteins cause defects in actin organization and vesicle targeting in the yeast *Saccharomyces cerevisiae*. FEBS Lett. *460*, 411–416.

Sambrook, J., and Russel, D. (2001). Molecular Cloning: a Laboratory Manual, Cold Spring Harbor, NY: Cold Spring Harbor Laboratory Press.

Schiestl, R. H., and Gietz, R. D. (1989). High efficiency transformation of intact yeast cells using single stranded nucleic acids as a carrier. Curr. Genet. *16*, 339–346.

Sciorra, V. A., Audhya, A., Parsons, A. B., Segev, N., Boone, C., and Emr, S. D. (2005). Synthetic genetic array analysis of the PtdIns 4-kinase Pik1p identifies components in a Golgi-specific Ypt31/rab-GTPase signaling pathway. Mol. Biol. Cell *16*, 776–793.

Shevchenko, A., Jensen, O. N., Podtelejnikov, A. V., Sagliocco, F., Wilm, M., Vorm, O., Mortensen, P., Shevchenko, A., Boucherie, H., and Mann, M. (1996). Linking genome and proteome by mass spectrometry: large-scale identification of yeast proteins from two dimensional gels. Proc. Natl. Acad. Sci. USA *93*, 14440–14445.

Shevchenko, A., Schaft, D., Roguev, A., Pijnappel, W. W., Stewart, A. F., and Shevchenko, A. (2002). Deciphering protein complexes and protein interaction networks by tandem affinity purification and mass spectrometry: analytical perspective. Mol Cell Proteomics *1*, 204–212.

Soetens, O., De Craene, J. O., and Andre, B. (2001). Ubiquitin is required for sorting to the vacuole of the yeast general amino acid permease, Gap1. J. Biol. Chem. *276*, 43949–43957.

Strahl, T., Hama, H., DeWald, D. B., and Thorner, J. (2005). Yeast phosphatidylinositol 4-kinase, Pik1, has essential roles at the Golgi and in the nucleus. J. Cell Biol. *171*, 967–979.

Szivak, I., Lamb, N., and Heilmeyer, L. M. (2006). Subcellular localization and structural function of endogenous phosphorylated phosphatidylinositol 4-kinase (PI4K92). J. Biol. Chem. *281*, 16740–16749.

Tzivion, G., and Avruch, J. (2002). 14-3-3 proteins: active cofactors in cellular regulation by serine/threonine phosphorylation. J. Biol. Chem. *277*, 3061–3064.

van Heusden, G. P., and Steensma, H. Y. (2006). Yeast 14-3-3 proteins. Yeast *23*, 159–171.

Vasara, T., Keranen, S., Penttila, M., and Saloheimo, M. (2002). Characterisation of two 14-3-3 genes from *Trichoderma reesei*: interactions with yeast secretory pathway components. Biochim. Biophys. Acta *1590*, 27–40.

Vieira, O. V., Verkade, P., Manninen, A., and Simons, K. (2005). FAPP2 is involved in the transport of apical cargo in polarized MDCK cells. J. Cell Biol. *170*, 521–526.

Walch-Solimena, C., Collins, R. N., and Novick, P. J. (1997). Sec2p mediates nucleotide exchange on Sec4p and is involved in polarized delivery of post-Golgi vesicles. J. Cell Biol. *137*, 1495–1509.

Walch-Solimena, C., and Novick, P. (1999). The yeast phosphatidylinositol-4-OH kinase pik1 regulates secretion at the Golgi. Nat. Cell Biol. *1*, 523–525.

Wang, B., Yang, H., Liu, Y. C., Jelinek, T., Zhang, L., Ruoslahti, E., and Fu, H. (1999). Isolation of high-affinity peptide antagonists of 14-3-3 proteins by phage display. Biochemistry *38*, 12499–12504.

Wang, Y. J., Wang, J., Sun, H. Q., Martinez, M., Sun, Y. X., Macia, E., Kirchhausen, T., Albanesi, J. P., Roth, M. G., and Yin, H. L. (2003). Phosphatidylinositol 4 phosphate regulates targeting of clathrin adaptor AP-1 complexes to the Golgi. Cell *114*, 299–310.

Wei, Y. J., Sun, H. Q., Yamamoto, M., Wlodarski, P., Kunii, K., Martinez, M., Barylko, B., Albanesi, J. P., and Yin, H. L. (2002). Type II phosphatidylinositol 4-kinase beta is a cytosolic and peripheral membrane protein that is recruited to the plasma membrane and activated by Rac-GTP. J. Biol. Chem. *277*, 46586–46593.

Weixel, K. M., Blumental-Perry, A., Watkins, S. C., Aridor, M., and Weisz, O. A. (2005). Distinct Golgi populations of phosphatidylinositol 4-phosphate regulated by phosphatidylinositol 4-kinases. J. Biol. Chem. *280*, 10501–10508.

Wong, K., Meyers, R., and Cantley, L. C. (1997). Subcellular locations of phosphatidylinositol 4-kinase isoforms. J. Biol. Chem. *272*, 13236–13241.

Yaffe, M. B. (2002). How do 14-3-3 proteins work?– Gatekeeper phosphorylation and the molecular anvil hypothesis. FEBS Lett. *513*, 53–57.

Yaffe, M. B., Rittinger, K., Volinia, S., Caron, P. R., Aitken, A., Leffers, H., Gamblin, S. J., Smerdon, S. J., and Cantley, L. C. (1997). The structural basis for 14-3-3, phosphopeptide binding specificity. Cell *91*, 961–971.

Yang, C. H., Lambie, E. J., Hardin, J., Craft, J., and Snyder, M. (1989). Higher order structure is present in the yeast nucleus: autoantibody probes demonstrate that the nucleolus lies opposite the spindle pole body. Chromosoma *98*, 123–128.